

NPS ARCHIVE
1960
KERTZ, J.

ERROR RATE CONTROL OF A SECOND-ORDER
SERVOMECHANISM WITH COULOMB
FRICTION AND BACKLASH

JACOB D. KERTZ

DUDLEY KNOX LIBRARY
NAVAL POSTGRADUATE SCHOOL
MONTEREY, CA 93943-6101

DUDLEY KNOX LIBRARY
NAVAL POSTGRADUATE SCHOOL
MONTEREY, CA 93943-5101

ERROR RATE CONTROL OF A SECOND-ORDER
SERVOMECHANISM WITH COULOMB FRICTION AND BACKLASH

* * * * *

JACOB D. KERTZ

ERROR RATE CONTROL OF A SECOND-ORDER
SERVOMECHANISM WITH COULOMB FRICTION AND BACKLASH

by

JACOB D. KERTZ

//

LIEUTENANT, UNITED STATES NAVY

Submitted in partial fulfillment of
the requirements for the degree of

MASTER OF SCIENCE

United States Naval Postgraduate School
Monterey, California

[1960]

1960

MECHANISM WITH COULOMB FRICTION AND WEIGHT

ERROR RATE CONTROL OF A SECOND-ORDER

by

JACOB D. KERTZ

LIEUTENANT, UNITED STATES NAVY

Submitted in partial fulfillment of
the requirements for the degree of

MASTER OF SCIENCE

United States Naval Postgraduate School
Monterey, California

ERROR RATE CONTROL OF A SECOND-ORDER
SERVOMECHANISM WITH COULOMB FRICTION AND BACKLASH

by

JACOB D. KERTZ

DUDLEY KNOX LIBRARY
NAVAL POSTGRADUATE SCHOOL
MONTEREY, CA 93943-5101

This work is accepted as fulfilling
the thesis requirements for the degree of
MASTER OF SCIENCE

ABSTRACT

Compensation for linear second-order servomechanisms has been used for many years to improve performance. This thesis studies in detail the use of error rate or derivative control as one method of improving performance. The effects of coulomb friction and backlash on the error rate control system are also studied. The error rate control system with coulomb friction and backlash were simulated on the Analog Computer to demonstrate qualitative results of this type of compensation. The favorable results of this investigation are then summarized in the conclusions.

The author wishes to express his appreciation for the suggestion of this thesis topic and the invaluable aid extended by Professor G. J. Thaler of the Electrical Engineering Department of the U. S. Naval Postgraduate School.

TABLE OF CONTENTS

Section	Title	Page
I.	General Introduction to the Problem	1
II.	Error Rate Control	15
1.	ERC With Step Inputs	
A.	Basic Servomechanism	16
B.	Servo with Coulomb Friction	19
C.	Servo With Backlash	21
D.	Servo with Coulomb Friction and Backlash	24
2.	ERC With Ramp Inputs	
A.	Basic Servomechanism	28
B.	Servo With Coulomb Friction	30
C.	Servo With Backlash	32
D.	Servo With Coulomb Friction and Backlash	33
III.	Analog Computer Simulation of an ERC Servomechanism	34
IV.	Conclusions	50
V.	Bibliography	52
VI.	Appendix	53

LIST OF ILLUSTRATIONS

Figure		Page
1.	Proportional-Error Servomechanism	1
2.	Standard Servomechanism Inputs	2
3.	Backlash	7
4.	Phase Trajectory	8
5.	Ramp Input With Coulomb Friction	10
6.	Phase Trajectory of a Second-Order Servomechanism With Coulomb Friction and Backlash for a Ramp Input	12
7.	Representative Transient Response	15
8.	Servomechanism With Error Rate Control	16
9.	Error Rate Control Servomechanism	18
10.	Effect of ERC for the Same Damping Ratio	20
11.	Servomechanism With Backlash	21
12.	Phase Trajectory of an ERC Servo With Backlash	22
13.	Servo With Backlash, Coulomb Friction on the Motor Shaft	25
14.	Servo With Backlash, Coulomb Friction on the Load Shaft	27
15.	ERC Servomechanism With Ramp Input	29
15a.	Ramp Input on an ERC Servo With Coulomb Friction	31
16.	Block Diagram of the Second-Order Servomechanism With Backlash and Coulomb Friction	34
17.	Analog Simulation Circuit for the Error Rate Control System	35
18.	Step Inputs Into Basic Servomechanisms	38
19.	Step Input With Backlash and Coulomb Friction	39

LIST OF ILLUSTRATIONS

Figure		Page
20.	Phase Plane Plot for Step Inputs With Backlash and Coulomb Friction	40
21.	Step Input With Backlash	41
22.	Step Input With Backlash	43
23.	Small Step Input With Coulomb Friction	44
24.	Ramp Input With Coulomb Friction	45
25.	Ramp Input With Backlash	47
26.	Ramp Input With Backlash and Coulomb Friction	48
27.	Phase Plane Plot for Ramp Inputs With Backlash and Coulomb Friction	49

TABLE OF SYMBOLS

Δ	Backlash
C	Coulomb Friction
ξ	Error in position
$\dot{\xi}$	Error rate
f	Viscous friction coefficient
J	Moment of inertia
K_1	Error torque constant
K_2	Error rate torque constant
ω_i	Input velocity
ω_n	Undamped natural angular velocity
t	Time
$\bar{\theta}$	Bar on top indicates computer value
θ_i	Input position
$\dot{\theta}_i$	Input velocity
$\ddot{\theta}_i$	Input acceleration
θ_o	Output position
$\dot{\theta}_o$	Output velocity
$\ddot{\theta}_o$	Output acceleration
ρ	Damping ratio

1. GENERAL INTRODUCTION TO THE PROBLEM.

This thesis is concerned with the problem of analyzing the performance of a piecewise linear servomechanism with Error Rate or Derivative control. The added effects of coulomb friction and backlash are also considered.

The word "servomechanism" as used in this thesis is defined as a closed loop automatic control system which specifically controls an output position. The primary purpose of any servomechanism is to drive an output load in such a manner so that its position at all times corresponds to that of the input member of the system. Practical systems can only approach this ideal due to the effects of friction, inertia and various types of non-linearities such as backlash, stiction, coulomb friction, saturation, etc.

An example of a simple closed loop servomechanism is as follows:

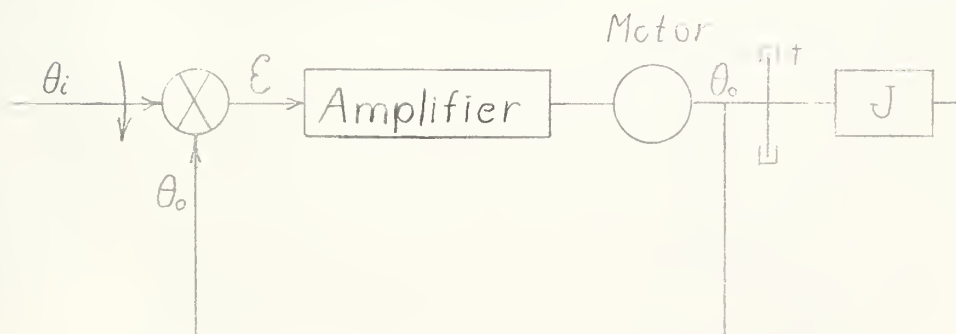


Fig. 1. Proportional-Error Servomechanism.

The differential equations of this system are:

$$J\ddot{\theta}_i = \tau_i - f\dot{\theta}_i \quad (1)$$

τ_i is assumed to be equal to the $K_1 \mathcal{E}$ where K_1 is the torque constant of the motor. The equation of the system can then be written as

$$J \frac{d^2 \mathcal{E}}{dt^2} + f \frac{d \mathcal{E}}{dt} = K_1 \mathcal{E} \quad (2)$$

where $\mathcal{E} = \theta_i - \theta_o$.

The solution to this equation can be solved in terms of either θ_o or \mathcal{E} since they are equivalent. Since error is normally the item in which we are most interested, all solutions in this thesis will be in terms of \mathcal{E} rather than θ_o .

In order to compare the responses of various systems, it is desirable to choose an input function of known characteristics, and apply it to all systems. The step and ramp inputs are used throughout this work. They are represented graphically in Fig. 2.

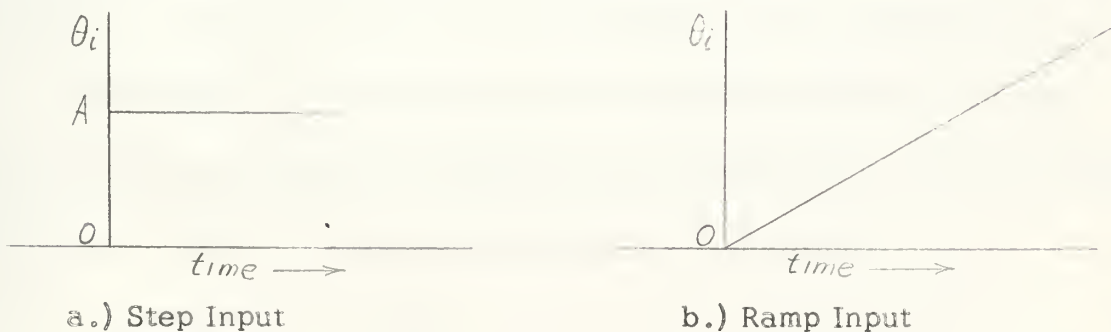


Fig. 2. Standard Servomechanism Inputs

The solution of equation 2 for a step input is:

$$\mathcal{E} = A \left[\left(\frac{1}{2} + \frac{Jf}{4J\sqrt{K_1/J - f^2/4J^2}} \right) e^{(-f/2J - j\sqrt{K_1/J - f^2/4J^2})t} + \left(\frac{1}{2} - \frac{Jf}{4J\sqrt{K_1/J - f^2/4J^2}} \right) e^{(-f/2J + j\sqrt{K_1/J - f^2/4J^2})t} \right] \quad (3)$$

and for a ramp input:

$$\begin{aligned} \epsilon = & \frac{1}{K_1} + \frac{K_1}{J} t \\ & + \left(\frac{(1 + \frac{f^2}{2} J K_1) - j(\frac{f}{K_1} \sqrt{K_1 J} + \frac{f^2}{4} J)}{j^2 \sqrt{K_1 J} - \frac{f^2}{4} J^2} \right) e^{-(\frac{f}{2} J \pm j \sqrt{K_1 J} + \frac{f^2}{4} J) t} \\ & + \left(\frac{1 - \frac{f^2}{2} J K_1 - j(\frac{f}{K_1} \sqrt{K_1 J} - \frac{f^2}{4} J)}{j^2 \sqrt{K_1 J} - \frac{f^2}{4} J^2} \right) e^{-(\frac{f}{2} J \mp j \sqrt{K_1 J} - \frac{f^2}{4} J) t} \end{aligned} \quad (4)$$

Depending on the parameters for the particular system, the system may be overdamped, critically damped or underdamped. In considering the foregoing, the steady state and transient performance criteria for the servomechanism must be considered.

The most important steady state criteria of performance in a position servomechanism is, of course, accuracy. Perfect accuracy is of course desired, but all systems have some imperfections that affect accuracy as well as some built in factors that affect accuracy. The maximum degree of error is usually specified by the application of the servomechanism.

In any given servomechanism, the transient performance requirements are more varied than the steady state requirements, but are equally important. The basic transient performance criteria are:

1. Maximum overshoot
2. Speed of response.
3. Stability

Maximum overshoot is a function of the system damping. The case in which there is zero overshoot is known as the critically damped case

and occurs when $K_1/J = f^2/4J^2$. The amount of damping with respect to the critical damping is usually expressed in the form of a dimensionless damping ratio, ζ .

$$\text{where} \quad \zeta \triangleq \frac{f}{f_c},$$

$$f_c \triangleq 2\sqrt{K_1 J}.$$

Therefore
$$\zeta = \frac{f}{2\sqrt{K_1 J}}.$$

It is also convenient to use ratio

$$\omega_n = \sqrt{K_1/J}$$

which is the undamped natural angular velocity. These two parameters can then be substituted in equations 3 and 4, thereby reducing the number of system constants from three to two. These equations simplify to the following for the underdamped case:

$$\mathcal{E} = A \left(\frac{e^{-\zeta \omega_n t}}{\sqrt{1-\zeta^2}} \right) \sin(\sqrt{1-\zeta^2} \omega_n t + \psi) \quad (5)$$

$$\text{where } \psi = \tan^{-1} \sqrt{1-\zeta^2} / \zeta.$$

$$\mathcal{E} = \frac{2\zeta \omega_n}{\omega_n} \left[1 - \frac{e^{-\zeta \omega_n t}}{2\zeta \sqrt{1-\zeta^2}} \sin(\sqrt{1-\zeta^2} \omega_n t + \psi) \right] \quad (6)$$

$$\text{where } \psi = \tan^{-1} 2\zeta \sqrt{1-\zeta^2} / (2\zeta^2 - 1)$$

The overdamped case where $\zeta > 1$ has few practical uses since this results in a very slow system. The critical damped case where $\zeta = 1$ has the fastest response without overshoot. The usual requirements, however, are to approach the desired position within a specified tolerance in the shortest practical time. This is accomplished by the use

of an underdamped system where $\zeta < 1$. The use of an underdamped system results in an overshoot of the steady state condition and a transient oscillation occurs. The first overshoot is always the greatest and its maximum value is of course termed the maximum overshoot. Any undesirable features which result from overshooting will, therefore, result in major part from the first overshoot and the succeeding overshoots will be of lesser importance. It thus becomes important to know what undesirable features result from overshooting and the limitations which must be placed on the peak overshoot. The two basic objections to large overshoot are: (1) The possibility of damage to the system which may result from the large acceleration inherent in a system with a large peak overshoot, and (2) the slowness with which a badly underdamped system approaches steady state. Experience has indicated that satisfactory performance is more frequently obtained when the maximum overshoot is limited to 1.5 of the command signal. Generally a ζ in the range .2 to .8 gives satisfactory performance.

The speed of response depends on the factor $e^{-\zeta \omega_n t}$ which is a multiplier of all underdamped systems. The product $\zeta \omega_n$ should be large for a high speed response. Since $\zeta \omega_n = \frac{f}{2\sqrt{K_1 J}} \sqrt{K_1/J} = \frac{f}{J}$

it can be seen that due to the limitation on ζ for overshoot, only limited adjustment of the speed of response can be obtained through an increase in f , since it is usually difficult to decrease J . However, a relative increase in speed of response can be obtained if K_1 is increased since this results in a faster, but more oscillatory system. The practical

limitation on increasing K_1 is the allowable overshoot and the specified tolerance on correspondence.

A criterion of great importance in considering transient behavior is the stability of the system. Because of the feedback loop, it is entirely possible for the system to hunt continuously (i.e., be unstable or have a limit cycle) if the system has been improperly designed. It is to be noted that a stable system will also oscillate if it is not in proper adjustment, but the preceding statement refers to a servomechanism which is impossible to stabilize by adjustment. With but few exceptions, specifications require that a servomechanism be stable.

For the simple proportional-error servomechanism, the steady state error for a step input can readily be seen to be zero from equation 5. The steady state error for a ramp input is equal to $2\phi\omega_i/\omega_n$, where ω_i is the input velocity. This reduces to $\phi\omega_i/K_1$ in the dimensional parameters. This error can be decreased by increasing K_1 but this makes the system more oscillatory. The amount that ϕ can be reduced is limited by practical considerations.

It can be seen that the specifications under which a servomechanism are constructed are often conflicting. That is, the specifications may demand for example, that the velocity lag error with a ramp input be .1 radian or less. The satisfaction of the foregoing may require that the gain be set so high as to result in a grossly underdamped system, and this would violate the specification regarding the maximum peak overshoot.

Thus far, only a simple linear system has been considered. However,

most systems have non-linearities to various degrees which require additional equations to completely describe the system or possibly some form of graphical solution for non-linearities which cannot be described by mathematical equations. The non-linearities considered in this thesis are coulomb friction and backlash. Coulomb friction is a constant drag or reaction force which is independent of velocity and will cause a moving system to stick or stop abruptly when the driving force drops below the coulomb friction force. The coulomb friction effect is present when the system is motionless, and sufficient drive force must be applied to overcome this friction force if motion is to be initiated.

The effect of backlash is shown in Fig. 3, which indicates that a dead space is created, i.e., the adjacent gear teeth must move through a finite distance before making contact with each other. This phenomenon is not particularly bothersome as long as unidirectional operation is expected, but reversals in direction require that the backlash be taken up each time. This is sometimes noisy and bothersome in operation, and can cause instability in feedback control systems.

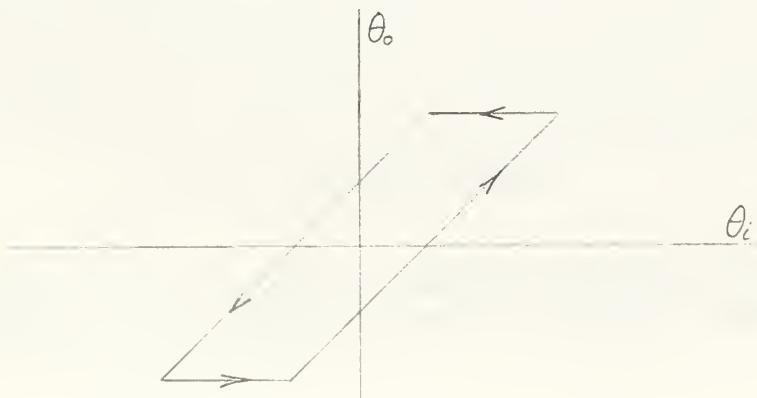


Fig. 3. Backlash.

The torque equilibrium equation for a second-order proportional error servomechanism with coulomb friction reacting to a step displacement input is:

$$J\ddot{\epsilon} + f\dot{\epsilon} + K_1\epsilon + C \operatorname{sign} \dot{\epsilon} = 0 \quad (7)$$

The isocline equation of this system is:

$$\dot{\epsilon} = \frac{-K_1\epsilon}{NJ + f} - \frac{C}{NJ + f} \quad (7a)$$

where N is the slope of the phase trajectory where it crosses the designated isocline. Equation 7a is the equation of two families of straight lines in the ϵ versus $\dot{\epsilon}$ plane emanating from as shown in Fig. 4.

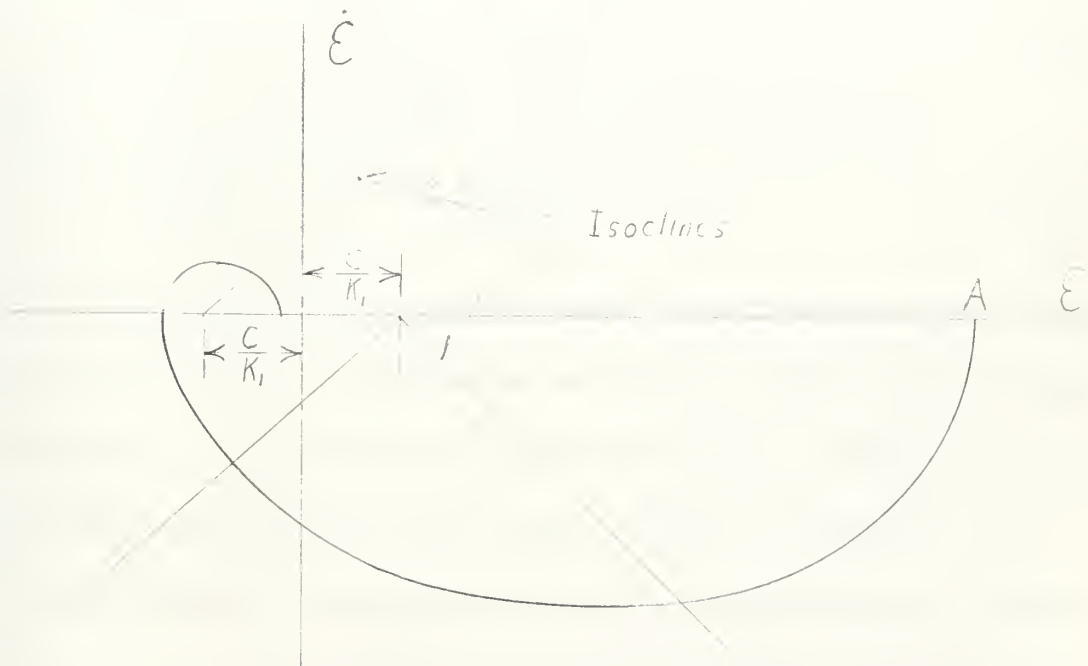


Fig. 4. Phase Trajectory

¹M. P. Pastel and G. J. Thaler, "Stability Criteria for Instrument Servomechanism with Coulomb Friction and Stiction," Applications and Industry, November 1959.

These isoclines are identically the isoclines of the linear system (without C) except for a translation of the upper and lower half planes with respect to the origin. For a step displacement input to initiate motion, it is apparent from equation 7 that the amplitude of the step must be such that \mathcal{E} is greater than C/K_1 . The trajectory then follows the path dictated by the isocline until it terminates on the \mathcal{E} axis between the foci. Coulomb friction is always stabilizing when a step displacement input is used, however, there is always some static error.

When a ramp function is applied to the servomechanism with coulomb friction, the following equation applies.

$$J\ddot{\mathcal{E}} + f\dot{\mathcal{E}} + K_1\mathcal{E} = f\omega_i + C \operatorname{sign}(\dot{\theta}_i - \dot{\mathcal{E}}) \quad (8)$$

where $\omega_i = \dot{\theta}_i$ = input velocity. The isocline equation is:

$$\dot{\mathcal{E}} = -\frac{K_1\mathcal{E}}{NJ+f} + \frac{f\omega_i + C \operatorname{sign}(\dot{\theta}_i - \dot{\mathcal{E}})}{NJ+f} \quad (8a)$$

Equation 8a defines two families of radial lines intersecting the \mathcal{E} axis at $\mathcal{E} = (f\omega_i \mp C)/K_1$. The foci are separated by $2C/K_1$, but the origin of coordinates is not midway between these foci, it is displaced from this mid-point by an amount $f\omega_i/K_1$. Also, the term $C \operatorname{sign}(\dot{\theta}_i - \dot{\mathcal{E}})$ designates the set of isoclines to be used, and thus defines a dividing line at $\dot{\mathcal{E}} = \omega_i$. This is shown in Fig. 5 for an arbitrarily selected ω_i .

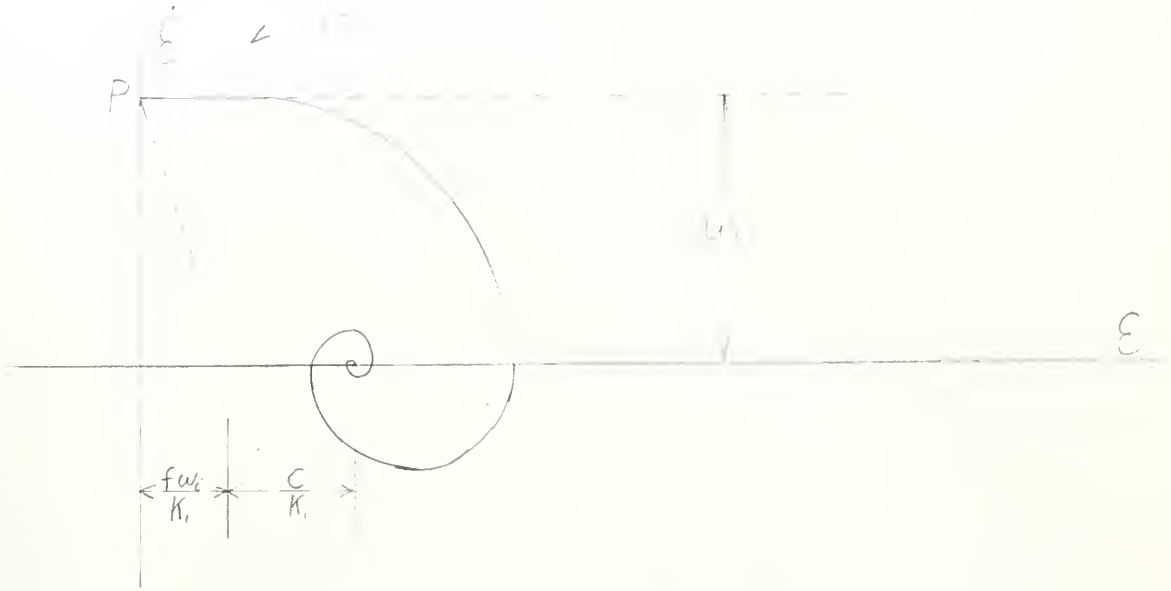


Fig. 5. Ramp input with coulomb friction.

The phase trajectory for a ramp input has initial conditions $\varepsilon = 0, \dot{\varepsilon} = \omega_c$, and thus starts at point P . Motion is initiated when $K_1 \varepsilon = C$, corresponding to a horizontal displacement from point P of amount $\varepsilon = C/K_1$. This is precisely the point at which the $N = 0$ isocline crosses the dividing line. After one complete spiral about the focus, the trajectory must cross the $N = 0$ isocline below the dividing line if the linear system has $\zeta > 0$. The phase trajectory spirals into the focus and the steady-state condition provides a velocity lag error.

$$\varepsilon_{ss} = (f\omega_c + C)/K_1 \quad (9)$$

Note that the phase plane of Fig. 5 is for only one input velocity.

For each new ω_c the dividing line and origin must be shifted.

For a step input, the case in which the load inertia is very small compared to the motor inertia, backlash causes the following sequence

elements to happen. The motor drives (with backlash taken up) reducing the error, as the motor velocity decreases, the load velocity also decreases, and continuous mechanical contact is maintained because $\dot{J}_L \sim \dot{\theta}$ and friction provides drag on the output. When the motor velocity becomes zero the load velocity also becomes zero. If the error is not zero the motor reverses but the load does not move because of the backlash. Thus the error does not change and the motor is driven open-loop with a constant driving torque until the backlash is taken up. The load is then "picked up" by the drive and both the output velocity and the error rate jump from zero to the instantaneous drive shaft velocity. This sequence is usually repeated a number of times.

It is well known that the effect of backlash is destabilizing. The net result of the condition described above is certainly a step response with extended duration of oscillation and may result in a limit cycle, or in a static error. Which of these alternatives exists on the viscous damping ratio, ζ , as is shown in Thaler's and Pastel's paper.¹

Backlash in a system with a small load inertia and coulomb friction on the motor shaft is destabilizing. The backlash must be taken up before the output can move. This results in an increase in the initial error before the system can move. This initial error is:

$$\epsilon_{\text{initial}} = C/K_t + \Delta. \quad (10)$$

¹M. P. Pastel and G. J. Thaler, "Instrument Servomechanism with Backlash Coulomb Friction and Stiction", AIEE Transactions Paper No. 60-118.

The system operates open loop according to the following equation until the backlash is taken up.

$$J\ddot{\theta}_M + f\dot{\theta}_M = \frac{K_1}{f}(\dot{x} - \dot{\theta}_M) \quad (11a)$$

This results in the motor position being given by:

$$\theta_M = \frac{\omega_i K_1}{f} \left[\frac{J}{f} \left(\frac{\dot{x}}{f} - \frac{J}{f} e^{-\frac{f}{J}t} - t \right) + \frac{t^2}{2} \right] \quad (11b)$$

Substituting the amount of backlash for θ_M gives the time it takes for the backlash period. At the end of the backlash period, the load is picked up by the motor at the speed obtained by inserting the value of t found from equation 11b in:

$$\dot{\theta}_M = \frac{\omega_i K_1}{f} \left[\frac{J}{f} \left(e^{-\frac{f}{J}t} - 1 \right) + t \right] \quad (11c)$$

After the load is picked up, the phase trajectory spirals into the focus as shown in Fig. 6. However, if the backlash is large, a limit cycle is

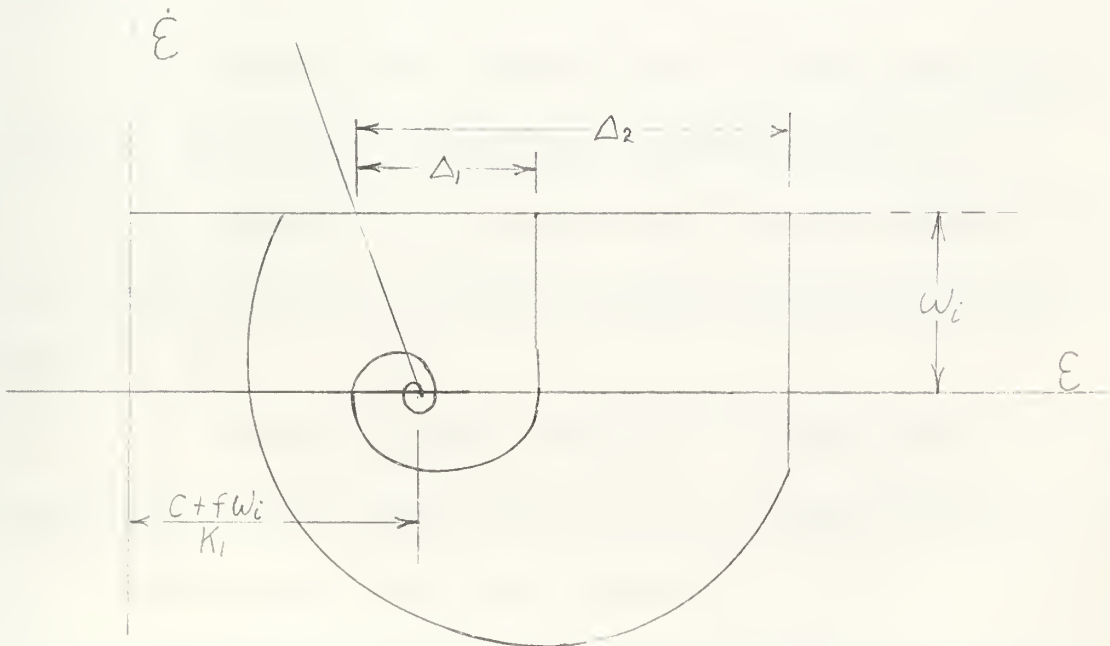


Fig. 6. Phase Trajectory of a second-order servomechanism with coulomb friction and backlash for a ramp input.

possible for low values of ω_1 . Fig. 6 shows values of ω_1 and backlash such that the phase trajectory is a spiral of such dimensions that it intersects the dividing line, the driving motor sticks, and a limit cycle is possible. However, any coulomb friction on the load shaft would stabilize the system once the backlash was taken up.

In the preceeding discussion, it has been apparent that there are some shortcomings in the use of a proportional error servomechanism. A few of these are enumerated below:

1. For a step input, the output torque is only directly proportional to the magnitude of the step, hence this results in poor performance for small errors.
2. The speed of response has only limited possibilities for adjustment due to the interrelation of ϕ and ω_1 and the undesirability of increasing f .
3. For a step input when coulomb friction is present, the system is unable to move unless the step input is greater than C/K_1 .
4. For a step input with coulomb friction, the steady state error can be anywhere from zero to $\pm C/K_1$. The value of K_1 is limited due to its effect on ϕ .
5. For a ramp input, motion is delayed on the output shaft until the error reaches a value greater than C/K_1 plus the value of backlash present.
6. The steady state error with a ramp input, $f\omega_c/K_1$ is difficult to reduce since this makes the system move oscillatory due to its effect on ϕ .

7. The possibility of a limit cycle with large values of backlash for step inputs when coulomb friction is present on the motor shaft.

The remainder of this thesis will outline and analyze one method of improving the performance of the second order servomechanism that has been discussed.

II ERROR RATE CONTROL

It is apparent from Part I, that some sort of modification or compensation of the basic proportional error system is needed. The problem of compensation, stated in its simplest terms is that of modifying the transient response of the system so that both steady state and transient specifications can be realized.

The form of compensation that this thesis analyzes is error rate or derivative control. A clear picture of error rate control can be obtained by a consideration of the underdamped response of a servomechanism. From the graphical picture and the differential equations of the system it is apparent that the envelope of the transient response is a function of the coefficient of viscous damping. The peak overshoot could be

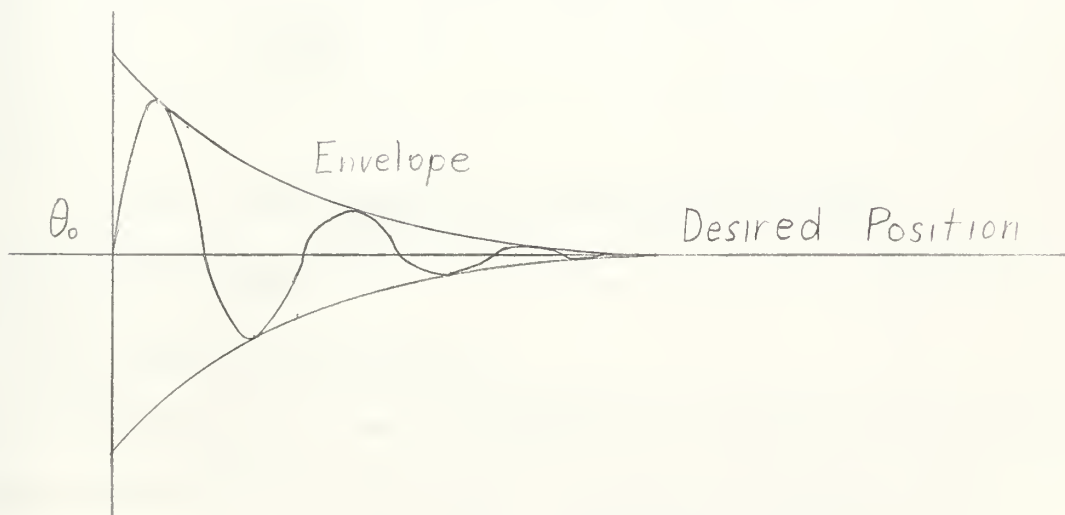


Fig. 7. Representative Transient Response

reduced by increasing the viscous damping, but this produces an undesired increase in the velocity lag error. However, from an examination of the curve; it can be seen that a correction which is a function of the

rate of change of error can be used to modify the transient response while at the same time leaving the steady state response unchanged. That is, in addition to the error signal, a signal which is the time derivative of the error signal is applied to the motor. In addition to the above stated advantages, it will become apparent during this development that there are other additional advantages to the use of error rate control.

A schematic of an error rate controlled servomechanism is shown in Fig. 8.

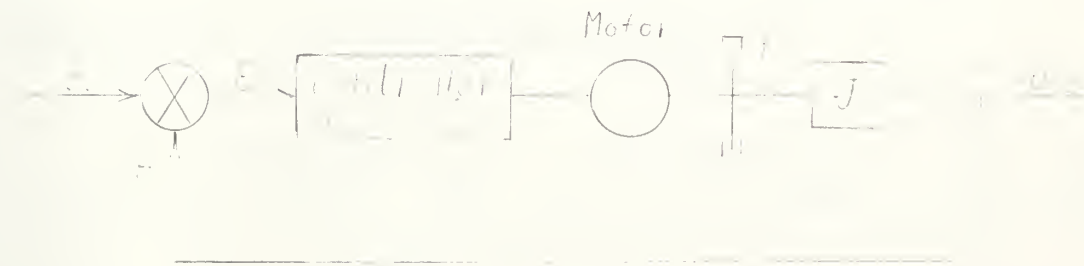


Fig. 8. Servomechanism with Error Rate Control

1. ERC With Step Inputs

A. Basic Servomechanism

The response of a servomechanism to a step input with error rate control (ERC) will now be outlined. The Laplace Transform method of solution of the linear differential equations will be used throughout this thesis. The system viscous friction and inertia will be assumed to be primarily in the motor, unless otherwise specified. For simplification of the equations, a one to one gear ratio will be used in this system.

The driving torque for an ERC system is:

$$T = A e^{-\zeta s} \quad (12)$$

and the equilibrium equation is then:

$$J\ddot{\theta} + f\dot{\theta} + K_2\theta = T \quad (13)$$

Writing the equilibrium equation in terms of θ and $\dot{\theta}$ results in:

$$\ddot{\theta} + \frac{f+K_2}{J}\dot{\theta} + \frac{K_1}{J}\theta = \ddot{\theta} + \frac{f+K_2}{J}\dot{\theta} \quad (14)$$

Let $f = f_0$ (step input)

then $\dot{\theta} = \delta(t)$ (an impulse)

and $\ddot{\theta} = \delta'(t)$ (a doublet).

Solving for θ in the Laplace notation gives

$$\theta = \frac{A(s + \frac{f}{J})}{s^2 + \frac{f+K_2}{J}s + \frac{K_1}{J}} = \frac{A(s + \frac{f}{J})}{s^2 + 2\zeta\omega_n s + \omega_n^2} \quad (15)$$

where $\zeta = \frac{f + K_2}{2\sqrt{K_1 J}}$.

Applying the initial value theorem to equation 15 gives the expected value of $\dot{\theta} = A$ at $t = 0$.

Solving for $\dot{\theta}$ gives the following:

$$\dot{\theta} = \frac{As(s + 2\zeta\omega_n)}{s^2 + 2\zeta\omega_n s + \omega_n^2} \quad (16)$$

Again applying the initial value theorem for $t = 0$.

$$\dot{\theta} = -A / J \quad (17)$$

This is a velocity that is directly proportional to the magnitude of the step input. This velocity is obtained instantly by the use of ERC. This can be explained by solving for the torque available at $t = 0$.

Fig. 8 shows a block diagram of an ERC servomechanism in transfer function notation



Fig. 9. Error Rate Control Servomechanism

It can be seen from the block diagram that:

$$\Theta = (Js^2 + f + K_2)s + K_1 \cdot \frac{f}{s} \quad (18)$$

This results in a transient solution of:

$$\theta = A_1 e^{s_1 t} + A_2 e^{s_2 t} + \frac{f}{s} \quad (19)$$

i.e. a pulse of infinite torque at $t = 0$. This infinite torque is what produces the finite velocity at $t = 0$.

Rewriting equation 14 in the isocline form produces the following equation since $\ddot{\theta}$ and $\dot{\theta}$ are zero for time greater than zero.

$$\dot{\epsilon} = \frac{-K_1/J}{1 + \frac{f+K_2}{J}} \epsilon = \frac{-AK_1}{1 + P(f+K_2)} \epsilon \quad (20)$$

It can be observed that the use of ERC with a step input changes the phase plane plot due to the pulse of infinite torque. This torque produces the initial value of $\dot{\epsilon} = -AK_1/J$. Whether or not this improves the performance of the system depends on the total damping, $(f + K_2) / \sqrt{1 + J}$. If the factor $(f + K_2)$ is held constant as K_2 is increased, the system response will be faster, but the peak overshoot will increase slightly

since the isoclines are unchanged. If $(f + K_2)$ is allowed to increase as K_2 is increased, the isoclines will be rotated counterclockwise due to the increased damping which will tend to reduce the overshoot and the speed of response. The ERC system will still be faster than that of a proportional system with a smaller ζ . The effect of ERC for the same damping factor is shown in Fig. 10.

B. Servomechanism with coulomb friction.

The addition of coulomb friction to the system of Fig. 8 changes the equilibrium equation to:

$$J \ddot{e} = f_0 + C \operatorname{sign} \dot{e} - K_1 e - K_2 \dot{e} \quad (21)$$

and for a step input this reduces to:

$$\ddot{e} + \frac{f + K_2}{J} \dot{e} + \frac{K_1}{J} e + \frac{C}{J} \operatorname{sign} \dot{e} = \frac{A}{J} u_0 t + \frac{f}{J} A \quad (22)$$

Writing this in the isocline form for $t > 0$:

$$\dot{e} = \frac{-\frac{K_1}{J} e - \frac{C}{J} \operatorname{sign} \dot{e}}{1 + 2\zeta \omega_n} \quad (23)$$

which is the equation of two families of straight lines radiating from

$e = \mp C/K_1$ and represents no change from the proportional error equations other than in the substitution of ζ for ξ .

Solving for e in the Laplace notation gives:

$$e = \frac{\frac{A}{J} (s + 2\zeta \omega_n)}{s^2 + 2\zeta \omega_n s + \omega_n^2} - \frac{\frac{C}{J} \operatorname{sign} \dot{e}}{s(s^2 + 2\zeta \omega_n s + \omega_n^2)} \quad (24)$$

where it can be readily seen that the addition of coulomb friction does not change the initial conditions of $e = A$ and $\dot{e} = -AK_2/J$. This is a major advantage of ERC as any step input, of any magnitude, will initiate



Fig. 10. Effect of ERC for the Same Damping Ratio

motion, regardless of the amount of coulomb friction present. However, there is no change in the steady state error as the limits of the termination error remain at $\pm C/K_1$. These limits however can represent a smaller actual error since K_1 can be increased with ERC while keeping the damping ratio constant by changes in f and K_2 .

C. Servomechanism with backlash.

Fig. 11 depicts schematically a servomechanism with backlash. The simplifying assumption is made that the inertia is entirely at the motor end of the backlash i.e. the case where the motor inertia is much larger than the load inertia referred to the motor shaft.

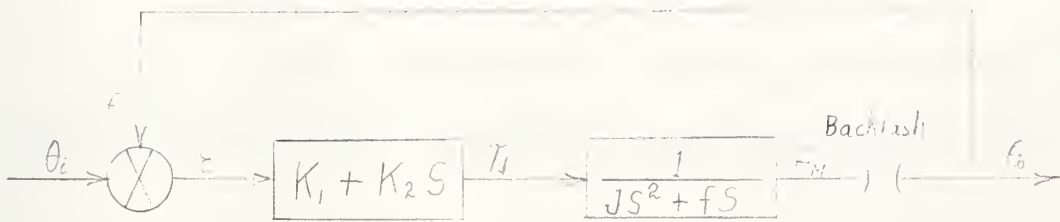


Fig. 11. Servomechanism with backlash

It is further assumed that the gears are making contact in the direction of motion at zero time. In this case equation 14 describes the motion.

$$\ddot{e} + \frac{f + K_2}{J} \dot{e} + \frac{K_1}{J} e = \ddot{\theta}_i + \frac{f}{J} \dot{\theta}_i \quad (14)$$

This gives the characteristic velocity jump of AK_2/J at $t = 0$ as shown in Fig. 12 from points A to B.

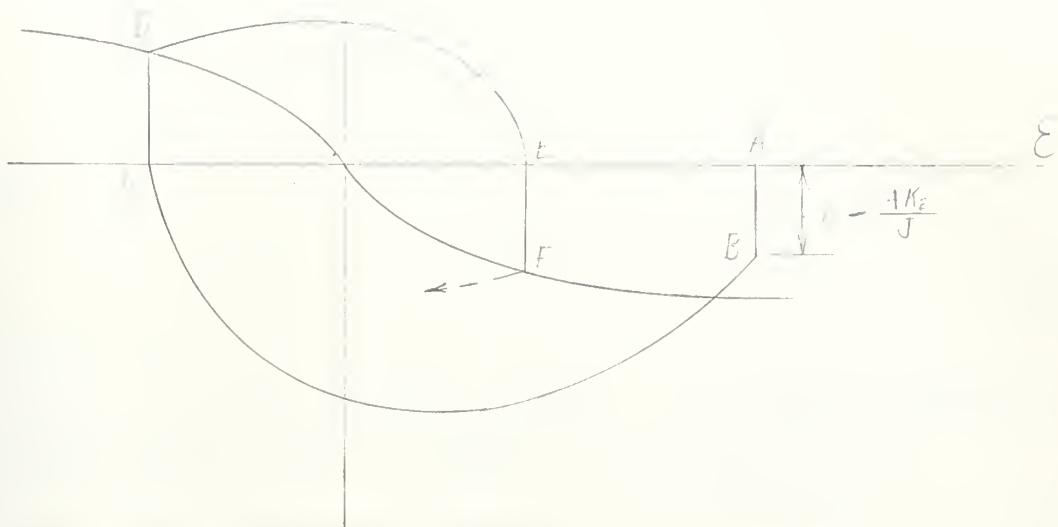


Fig. 12. Phase trajectory for an ERC servo with backlash.

From B to C the motion is described by the isocline form of equation 14.

$$\dot{\xi} = \frac{-\omega_n^2}{N + \xi^2 \omega_n^2} \xi \quad (20)$$

As point C is reached, the velocity changes sign, $\dot{\theta}_M$ tends to reverse and the gears open as the result of backlash. With the actuating signal remaining constant at ξ_C , the waveform of θ_M is determined from the differential equation and the boundary conditions.

$$J\ddot{\theta}_M + D\dot{\theta}_M = -K_E \xi_C \quad (25)$$

where $\xi = \xi_C$ and $\dot{\theta}_M = 0$ at $\theta_M = \theta_C$.

Therefore

$$\begin{bmatrix} t \\ 1 \end{bmatrix} = \begin{bmatrix} 1 & 0 \\ 0 & 1 \end{bmatrix} \begin{bmatrix} 1 \\ 1 \end{bmatrix} \quad (26)$$

$$\frac{\dot{\epsilon}_c}{4\dot{\epsilon}_m} = \left(-1 + \frac{2}{R} \gamma \alpha_m \right)$$

and

$$\frac{\dot{\epsilon}_c}{\dot{\epsilon}_m} = \frac{1}{2\gamma} \left(1 - C \right) \quad (27)$$

Equation 26 can be solved for t , letting ϵ_c equal the amount of backlash present. Then this value of t is used to solve for $\dot{\epsilon}_c$ from equation (27). During this backlash period ϵ and $\dot{\epsilon}$ do not change so the tracing point in Fig. 12 remains at C. At the end of the backlash period, the motor picks up the inertialess output shaft and:

$$\dot{\epsilon} = -\dot{\theta}_m \quad \dot{\theta}_c$$

at point D on Fig. 12. From D to E, equation 14 holds and the isocline equation (20) may be used for plotting the phase plane. This cycle then repeats itself. It can be seen that there are two backlash dividing lines, one the ϵ axis which is the separation line and the other a locus of points such as D and E which form a recombination line. This recombination line must be plotted point by point if the phase trajectory is to be constructed.

Backlash is always destabilizing and can cause a limit cycle to develop. The stability criteria as developed by Pastel and Thaler¹ indicates that the system is unstable (has a limit cycle) if $\xi_c \geq 0.29$. This is due to the presence of backlash, but independent of the amount of backlash. Thus a system with ERC may be stabilized by simply increasing the gain K_2 to increase ξ_c beyond the critical value of 0.29.

D. Servomechanism With Backlash and Coulomb Friction.

The addition of coulomb friction to the backlash problem discussed in the previous section has the typical stabilizing effect of coulomb friction, but the solution of the differential equations is dependent on where the coulomb friction is added, i.e. the load shaft or the motor shaft. The case of coulomb friction on the motor shaft will be considered first with the gears initially in contact. The equilibrium equation is:

$$\ddot{\xi} + \left(\frac{f + K_2}{J}\right)\dot{\xi} + \frac{K_1}{J}\xi + \frac{C}{J}\text{sign}\dot{\xi} = A(t) + \frac{f}{J} \quad (28)$$

which produces the characteristic jump in velocity of AK_2/J at $t = 0$.

The isocline equation is:

$$\dot{\xi} = \frac{-\omega_n^2}{N + 2\xi_c\omega_n}\xi - \frac{\frac{C}{J}\text{sign}\dot{\xi}}{N + 2\xi_c\omega_n} \quad (29)$$

This is the previously described two sets of radial lines with foci at $\pm C/K_1$ as shown in Fig. 13.

¹M. P. Pastel and G. J. Thaler, "Instrument Servomechanism With Backlash, Coulomb Friction and Stiction," AIEE Transactions Paper No. 60-118.

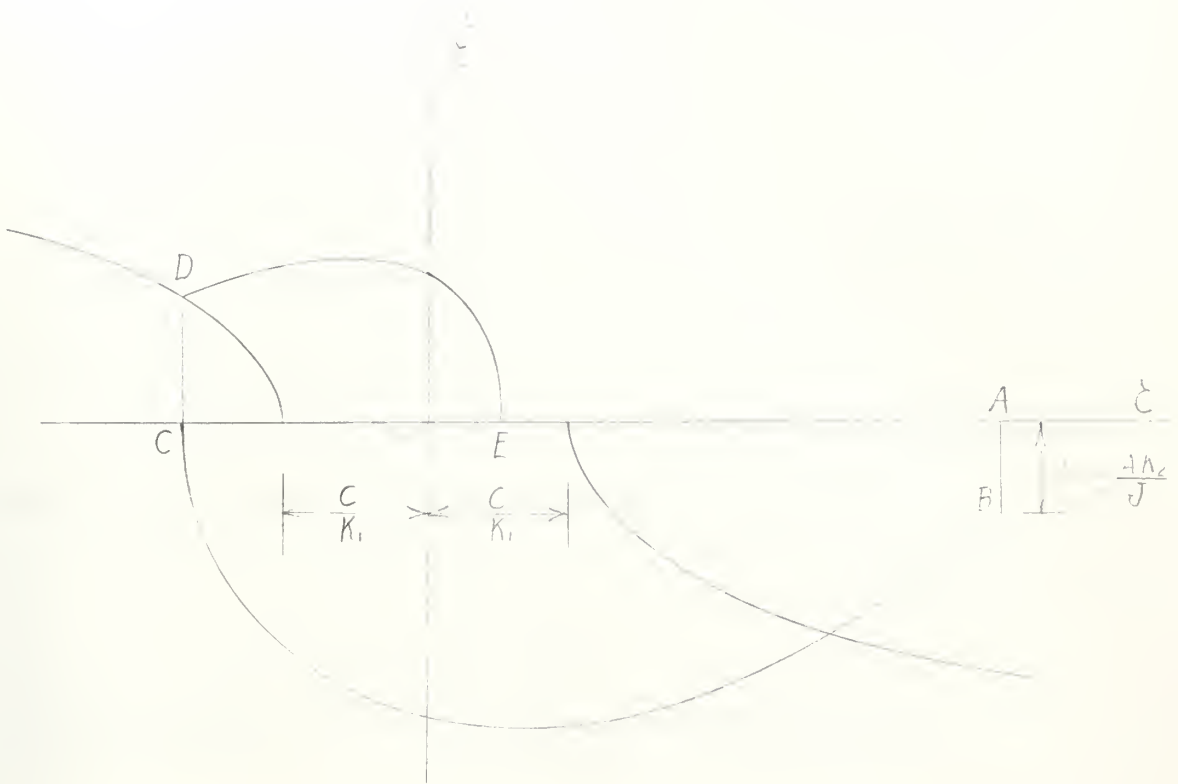


Fig. 13. Servo with backlash, Coulomb Friction on the motor shaft.

When point C is reached, the motor reverses and remains constant during the backlash period and the system motion is described by:

$$J\ddot{\theta}_M + f\dot{\theta}_M + C = 0 \quad (30)$$

where $\ddot{\theta}_M = \text{zero}$. Hence the backlash dividing line is also split and translated as shown in Fig. 13. During the backlash period:

$$\theta_M = (K_1 \epsilon_c - C_{\text{sign}} \dot{\theta}_M) \left[\frac{t}{f} + \frac{J}{f^2} \left(e^{-\frac{f}{J} t} - 1 \right) \right]$$

$$\dot{\theta}_M = \frac{\epsilon_c - \frac{C}{K_1} \text{sign} \dot{\theta}_M}{4 \zeta^2} \left(-1 + e^{-\frac{f}{J} t} + 2 \zeta e^{-\frac{f}{J} t} \right) \quad (31)$$

$$\frac{1}{P_3} \quad (32)$$

The method of solution for points along the recombination line is the same as that given in section C. It is apparent that if a trajectory terminates between the foci, the torque developed will be insufficient to initiate motion and a static error exists.

If the gears are separated at $t = 0$, equation 30 still holds but initial conditions at $t = 0+$ must be added, i.e. at $t (0+)$:

$$\begin{aligned} \epsilon &= 1 \\ \dot{\epsilon} &= -AK_2/J \end{aligned}$$

Then solving for θ_M in the Laplace notation results in:

$$\begin{aligned} \theta_M &= \frac{K_1 A - \text{sign} \dot{\theta}_M}{s^2 (1 + JS)} + \frac{AK_2}{(1 + JS)} \\ \epsilon_M &= (K_1 A - \text{sign} \dot{\theta}_M) \left(\frac{J}{f^2} \right) \left(e^{-\frac{f}{J}t} + \frac{f}{J}t - 1 \right) \end{aligned} \quad (33)$$

Solve equation 33 for t using ϵ_M equal to the initial backlash, if t is negative, it means motion starts instantly with $\dot{\epsilon} = -AK_2/J$. If t is positive solve equation 34 using this value of t .

$$\dot{\epsilon}_M = \frac{K_1 A - \text{sign} \dot{\theta}_M}{f} \left(1 - e^{-\frac{f}{J}t} \right) + \frac{AK_2}{J} e^{-\frac{f}{J}t} \quad (34)$$

then $\dot{\epsilon} = -\dot{\epsilon}_M = \dot{\theta}_0$ at the end of the backlash period. The remainder of the solution is as previously described.

When the coulomb friction is on the load shaft, assuming the gears are initially in contact, equations 28 and 29 describes the first part of the phase trajectory with the characteristic jump in velocity at $t = 0$ with the isocline radiating from the foci at $\pm C/K_1$. When the system stops at point C in Fig. 14 and the motor reverses the coulomb friction does not hold the motor shaft so that equation 25 applies.

$$J\ddot{\theta}_M + \dots = \dots \quad (25)$$

\dots is a constant during the backlash period, therefore \dots is zero. It is obvious that the backlash dividing line is not affected by the coulomb friction and goes through the origin. This is shown in Fig. 14.

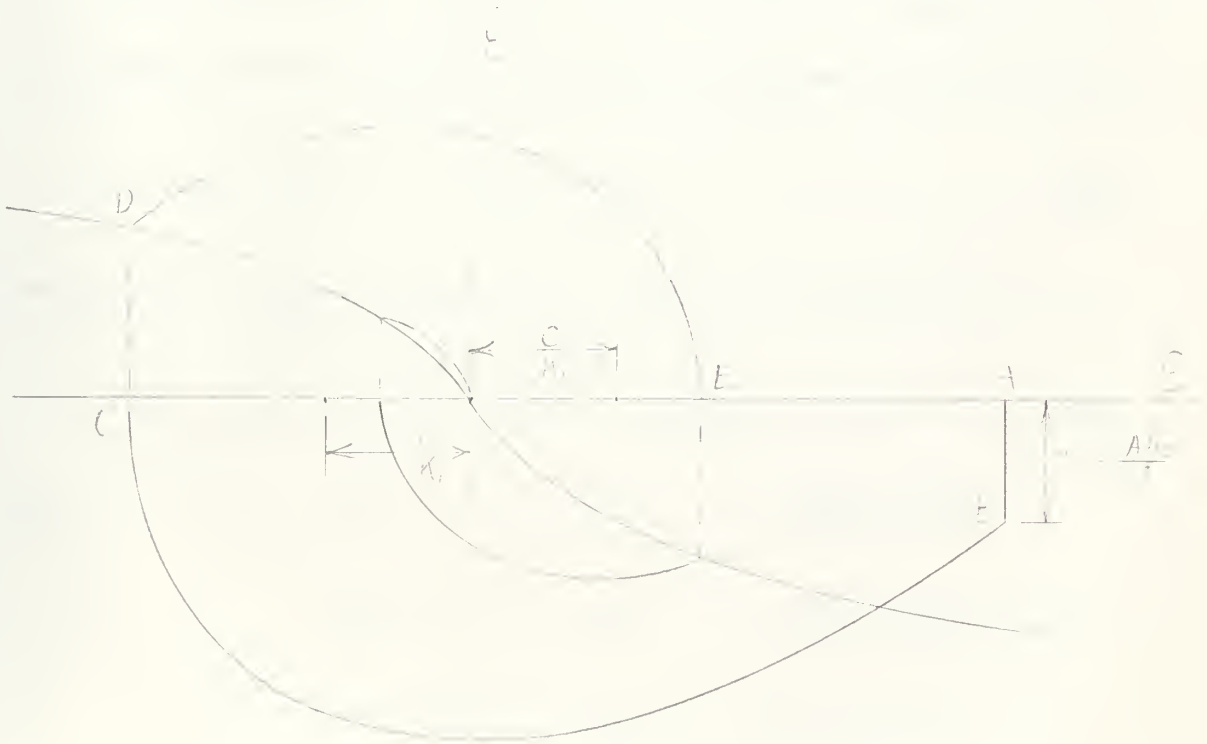


Fig. 14. Servo with backlash, Coulomb Friction on the load shaft.

The solution for the locus of the backlash recombination line is as described in section C. Fig. 14 shows that the coulomb friction is stabilizing and reduces the error to zero. Note that the phase trajectory which passes through the origin of the phase plane must lie on or inside the backlash recombination line or a static error results. ERC prevents the system from sticking for any step input as the impulse of torque is always able to provide the initial velocity. An ERC system does not require a threshold value of error as would be required by a proportional-error system to overcome the coulomb friction.

3. ERC With Ramp Inputs.

A. Basic Servomechanism.

The response of a servomechanism with ERC to a ramp input will now be considered. The basic equilibrium equation for the system is:

$$J\ddot{\theta}_e + f\dot{\theta}_e = T_1 - K_1\epsilon + K_2\dot{\epsilon} \quad (13)$$

Writing the equation in terms of θ_i and ϵ results in:

$$\ddot{\epsilon} + \frac{f+K_2}{J}\dot{\epsilon} + \frac{K_1}{J}\epsilon = \ddot{\theta}_i + \frac{f}{J}\dot{\theta}_i \quad (14)$$

Let $\theta_i = \omega_i t$ (ramp input)

$\dot{\theta}_i = \omega_i u(t)$ (step velocity input)

$\ddot{\theta}_i = \omega_i \delta(t)$ (an impulse)

These values substituted into equation 14 produce the following basic equation for ramp inputs:

$$\ddot{\epsilon} + \frac{f + k_2}{J} \dot{\epsilon} + \frac{k_1}{J} \epsilon = \frac{f}{J} \omega_i u(t) \quad (35)$$

Solving for ϵ in the Laplace notation gives:

$$\epsilon = \frac{\omega_i + \frac{f \omega_i}{J s}}{s^2 + \frac{f + k_2}{J} s + \frac{k_1}{J}} = \frac{\omega_i (s + 2 \zeta \omega_n)}{s (s^2 + 2 \zeta \omega_n s + \omega_n^2)} \quad (36)$$

Applying the final value theorem to equation 36 gives the steady state error.

$$\epsilon_{ss} = \frac{f \omega_i}{K_1}$$

The driving torque for an ERC system is $\tau_d = K_1 \epsilon + K_2 \dot{\epsilon}$,

at $t = 0+$, ϵ is zero and $\dot{\epsilon} = \omega_i$. Therefore there is an instantaneous torque available equal to $K_2 \omega_i$ whereas in a proportional-error system the torque is zero initially. The isocline equation is:

$$\dot{\epsilon} = \frac{-\omega_n^2}{N + 2 \zeta \omega_n} \epsilon + \frac{\omega_i u(t) + 2 \zeta \omega_n \omega_i u(t)}{N + 2 \zeta \omega_n} \quad (37)$$

Equation 37 defines a set of radial times emanating from $\epsilon = f \omega_i / K_1$.

This is illustrated in Fig. 15.

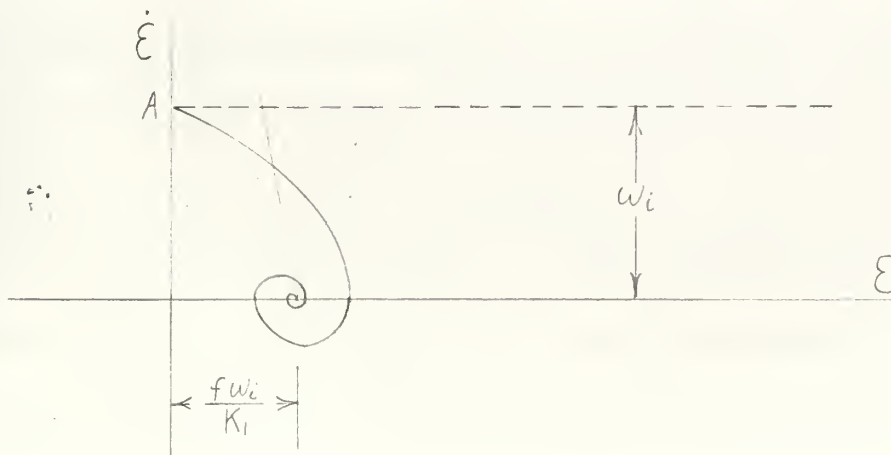


Fig. 15. ERC Servomechanism With Ramp Input.

The phase trajectory for a ramp input has initial condition of $\xi = 0$ and $\dot{\xi} = 0$ and thus starts at point A from which it spirals into the focus with the attendant velocity lag error of $f\omega_c/K_1$. The addition of ERC allows the steady state error to be reduced since K_1 can be increased as K_2 is increased.

B. Servo With Coulomb Friction.

When the input is a suddenly applied ramp function equation 38 applies.

$$\ddot{\xi} + \frac{f+K_2}{J} \dot{\xi} + \frac{K_1}{J} \xi = \frac{C}{J} \text{sign}(\dot{\theta}_i - \dot{\xi}) + \omega_c u_i(t) + \frac{f}{J} u_i(t). \quad (38)$$

For times greater than zero, the isocline equation is:

$$\dot{\xi} = \frac{-K_1/J}{N + \frac{f+K_2}{J}} \xi + \frac{\frac{C}{J} \text{sign}(\dot{\theta}_i - \dot{\xi}) + \frac{f}{J} \omega_c}{N + \frac{f+K_2}{J}}. \quad (39)$$

It can be seen from equation 38, that motion can only be initiated when

$$C \leq K_1 \xi + K_2 \omega_c$$

or that the minimum error before system movement must be:

$$\xi = (C - K_2 \omega_c) / K_1.$$

The effect of K_2 on the isoclines is illustrated in Fig. 15a. The $N = 0$ isocline is rotated counterclockwise, i.e. its slope = $-K_1/(f+K_2)$. The origin of coordinates moves in the same fashion as that of the proportional error system being dependent on values of ω_c . The intersection of the locus of the dividing line and the $\dot{\xi}$ axis with the slope of the $N = 0$ isocline determines the values of ω_c above which there is no delay in initiation of motion. The steady state error is not changed by ERC and is equal to: $\xi_{ss} = (C - K_2 \omega_c) / K_1$.

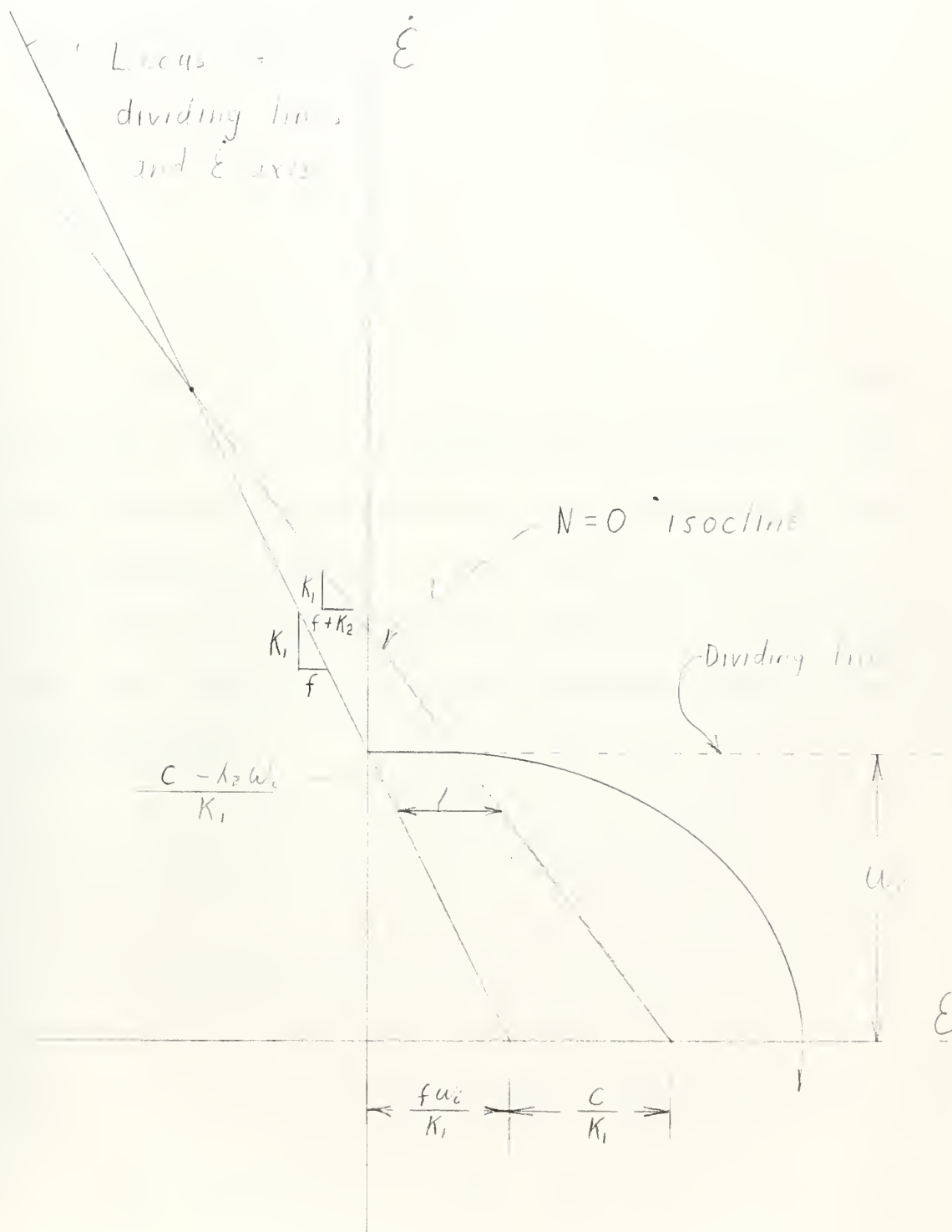


Fig. 15a. Ramp Input on an ERC Servo With Coulomb Friction

A large value of K_2 is desirable since this decreases the range of values of ϵ_1 which require an error before motion starts. A large K_2 also increased the factor $2\zeta\omega_n$ which provides rapid response and enables K_1 to be increased which reduces the steady state error while holding down the value of overshoot.

C. Servomechanism with Backlash

The effect of backlash on an ERC system is very similar to that described in section I for a proportional-error servomechanism. The basic difference is that the backlash is taken up faster due to the extra torque available from the $K_2 u_c$ term of the equilibrium equation. The value of the velocity jump on the phase plane at the end of the backlash period can be found from the following equations by letting ϵ_N equal the value of backlash.

$$A_N = \frac{\omega_c K_1}{f} \left[\frac{1}{f} + \frac{1}{\omega_c} \left(1 - \frac{f}{\omega_c} \right) \right] \quad (40)$$

$$+ \frac{\omega_c K_2 J}{f^2} \left(e^{-\frac{f}{J} t} + \frac{f}{J} t - 1 \right)$$

and

$$\dot{\epsilon}_N = \frac{\omega_c K_1 J}{f^2} \left[e^{-\frac{f}{J} t} + \frac{f}{J} t - 1 \right] \quad (41)$$

$$+ \frac{1}{f} \left(1 - e^{-\frac{f}{J} t} \right)$$

D. Servo With Coulomb Friction and Backlash.

The addition of backlash to a servo with the coulomb friction on the motor shaft presents the problem of a longer delay before the output shaft is placed in motion. Until the backlash period is over, the system operates open loop according to the following equations:

$$J\ddot{\theta}_M + f\dot{\theta}_M + C = 0, \quad \dot{\theta}_M = 0 \quad (42)$$

where $\dot{\theta}_M = 0$ and $\ddot{\theta}_M = 0$ for $t < t_1$ and $\dot{\theta}_M = K_1 \omega_c / f$ for $t > t_1$

for this period. Inserting these values in equation 42 reduces it to

$$J\ddot{\theta}_M + f\dot{\theta}_M = K_1 \omega_c L. \quad (43)$$

The solution to this is the same as for the proportional error case as shown in equations 11b and 11c. It takes just as long for the ERC system to take up the backlash as it did the proportional error system when coulomb friction is present. The ERC initiates motion sooner however due to the smaller time needed to overcome the coulomb friction. The possibility still exists for a limit cycle for large backlash and small ramp inputs. However this possibility is less than for the proportional error servo-mechanism due to the counterclockwise shifting of the $N = 0$ isocline. Again any coulomb friction on the output shaft would stabilize the system once the initial backlash was taken up.

III. Analog Computer Simulation of An ERC Servomechanism.

The previously described system was set up on a Donner Analog Computer to obtain some qualitative information as well as a feel for the error rate control servomechanism.

The block diagram of the simple second order system with backlash and coulomb friction is shown in Fig. 16.

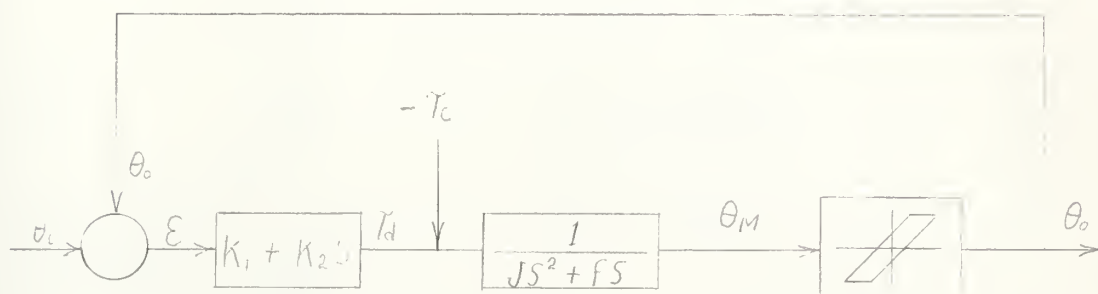


Fig. 16. Block diagram of the second order servomechanism with backlash and coulomb friction.

The actual simulation circuit used on the Analog Computer is shown in Fig. 17. The transfer function method was used in the simulations of the systems. This required the use of a differentiator which had many disadvantages. First, since the Donner computer is designed as a flexible machine, the differentiator network was difficult to stabilize since the amplifiers are designed also to be used as summing amplifiers and integrators. Second, the differentiating action tends to increase the "spikiness" of a varying input voltage, and hence tends to increase the chance of an overload. Third, and probably most important, the

differentiator tends to degrade the "signal-to-noise ratio" of the output voltage by amplifying the residual power-supply ripple and other higher-frequency disturbances which are always present to some extent.

The use of a step input causes an impulse in the differentiator and consequent overloading. The ideal impulse has an amplitude approaching infinity and lasts for an infinitesimal time, the product of amplitude and duration being finite. The practical impulse has finite amplitude and duration, but to give a reasonably close representation of an ideal impulse the duration must be short compared with the time constant of the system. To satisfy this requirement, it was necessary to saturate the amplifier on the differentiator. This saturation evidently affected the accuracy of the solution to some extent.

The parameters chosen for the simulated error rate control and proportional error servomechanism used were:

$$\xi = .3 = \xi_1$$

$$\omega_n = 1$$

$$A = .5 \text{ radian}$$

$$\omega_i = .04 \text{ radians / sec.}$$

$$\frac{K_2}{f} = .6$$

$$C = 1$$

$$\Delta = .05 \text{ radian}$$

The results of step inputs were investigated first. Due to a slight instability in the differentiator, it was necessary to add a small resistance in series with the capacitor on the differentiator. This resulted in a lead

transfer function of

$$\frac{e}{e_i} = - \frac{SR_c}{SR_c + 1}$$

instead of a true differentiation transfer function of

$$\frac{e_o}{e_i} = - SR_c$$

However since the added resistance and the capacitor was small, the RC product was very small and the solution was affected only slightly.

The transient solutions as recorded on the Brush Recorder are shown in Fig. 18 for the basic proportional error and error rate control servomechanisms. Fig. 19 shows the results of adding backlash and coulomb friction to these basic servomechanisms. Fig. 20 is the phase plane plots of the computer solutions of Fig. 19 as compared to the theoretical solutions. To plot the computer solutions, it was necessary to extrapolate the Brush Recorder traces of \dot{e} back into the saturated region. Since the slopes are well defined on the computer traces, this presented no problem. For the same damping ratio, it is to be noted that, the ERC system starts out with a higher velocity. However, the overshoot is slightly greater than for the proportional-error system. If the maximum overshoot were the main criteria, it could be reduced by increasing K_2 slightly.

Fig. 21 is the transient response for the ERC and proportional-error system with backlash alone. It is to be noted that a limit cycle develops for the ERC system while the proportional error system is stable. This limit cycle is probably due to the instability of the differentiator and according to the stability criteria should not exist for the $\zeta_1 = .3$ which

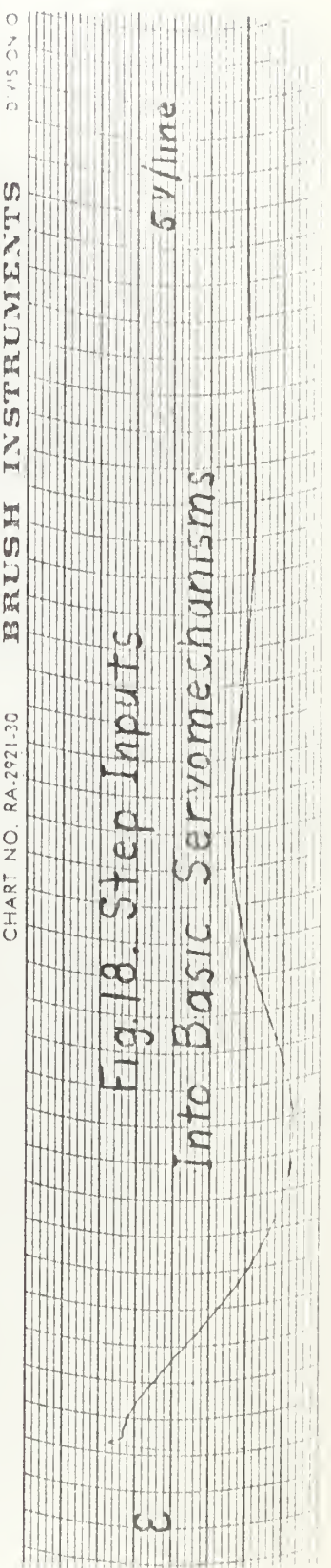
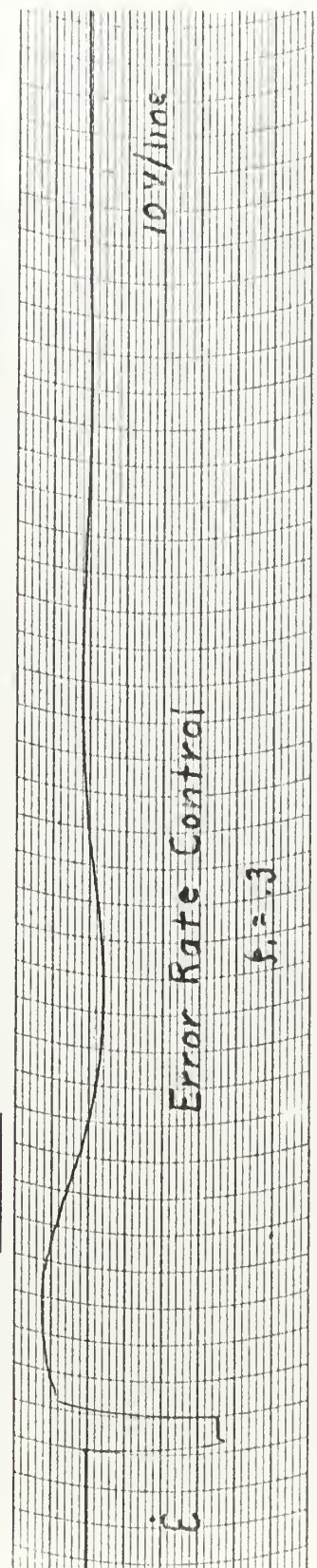
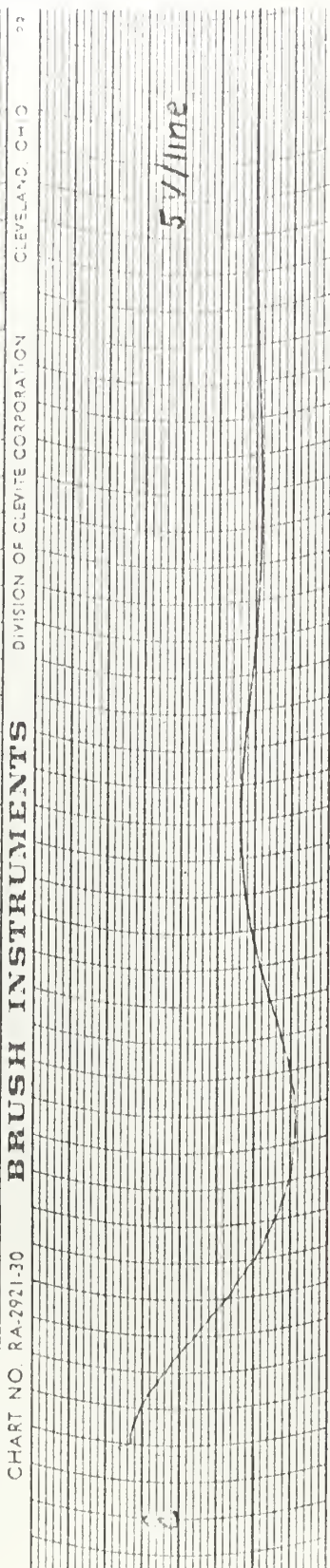
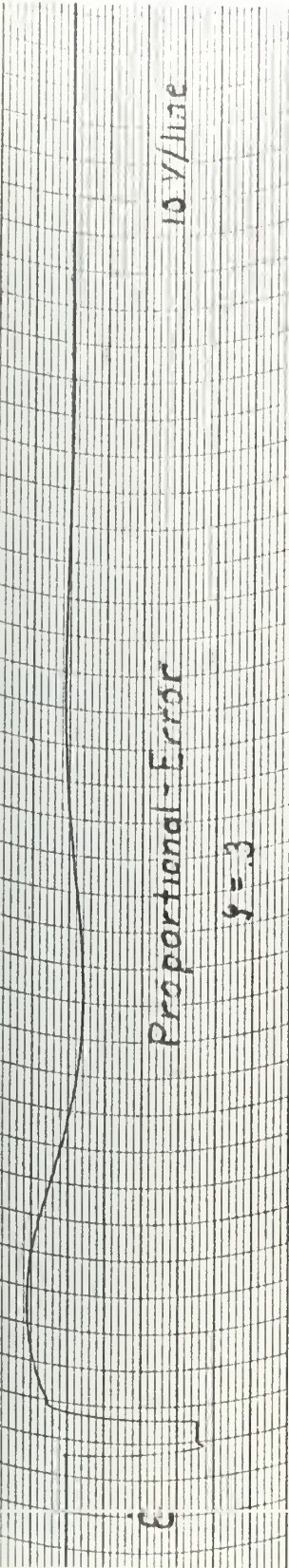


Fig. 18. Step Inputs
Into Basic Servomechanisms

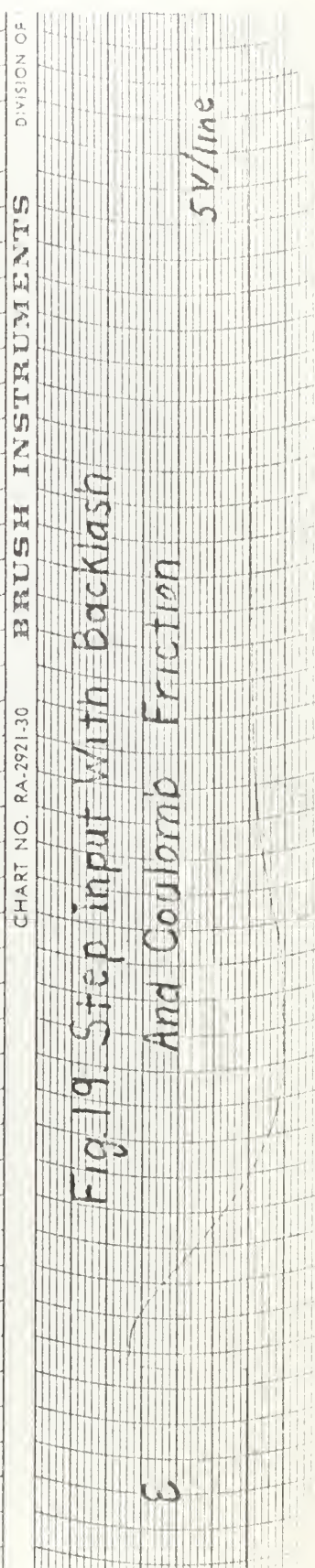
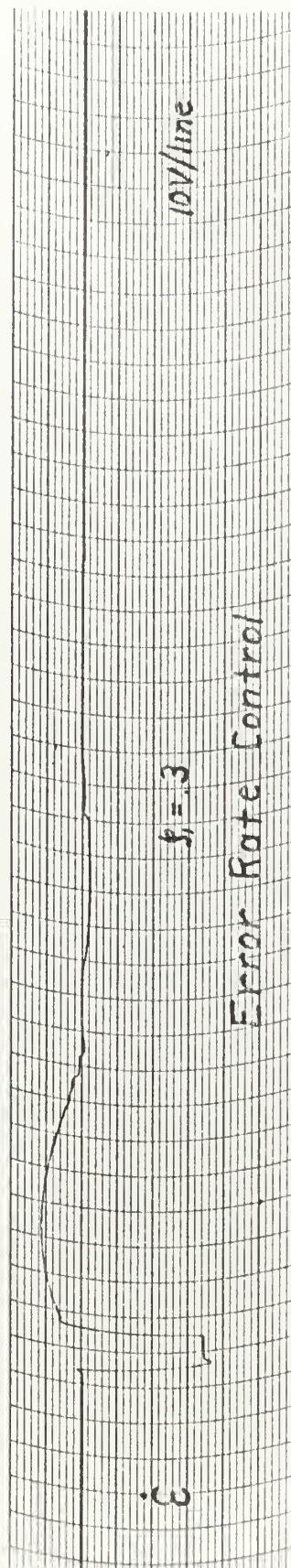
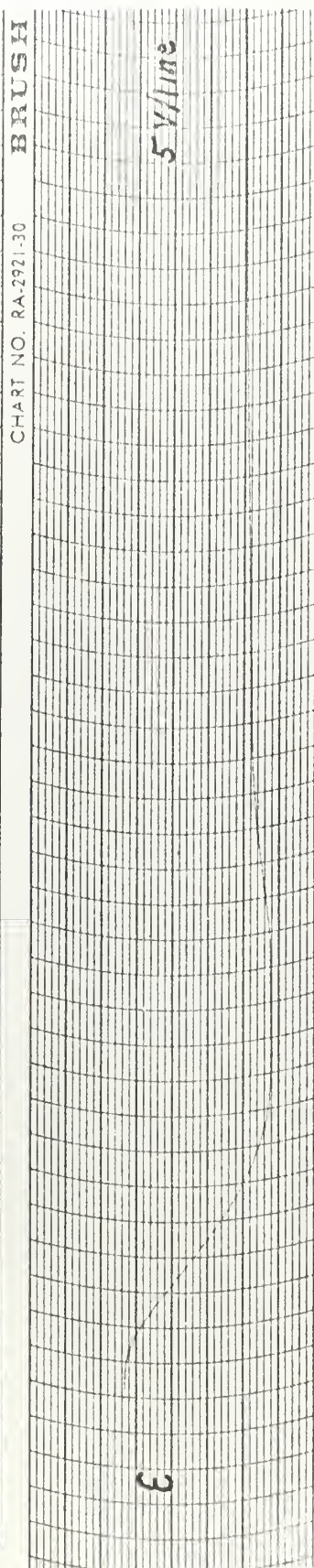
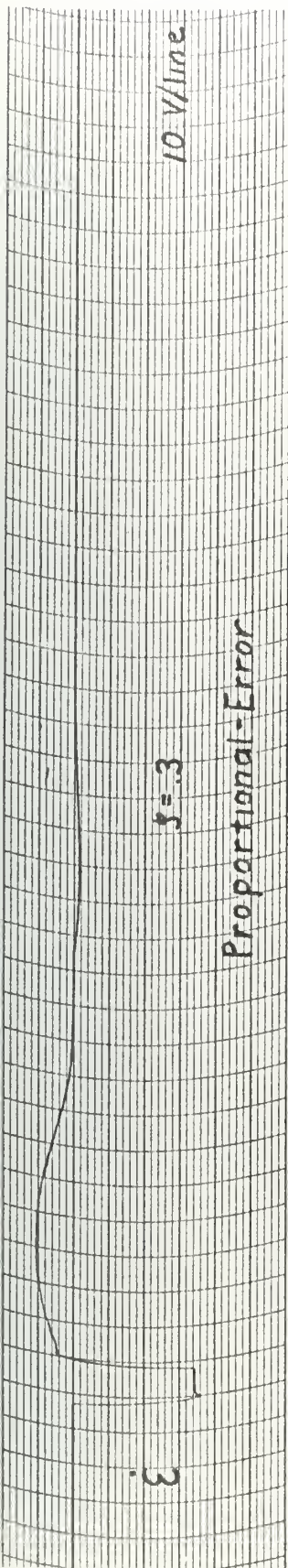


Fig. 19. Step input With Backlash
And Coulomb Friction

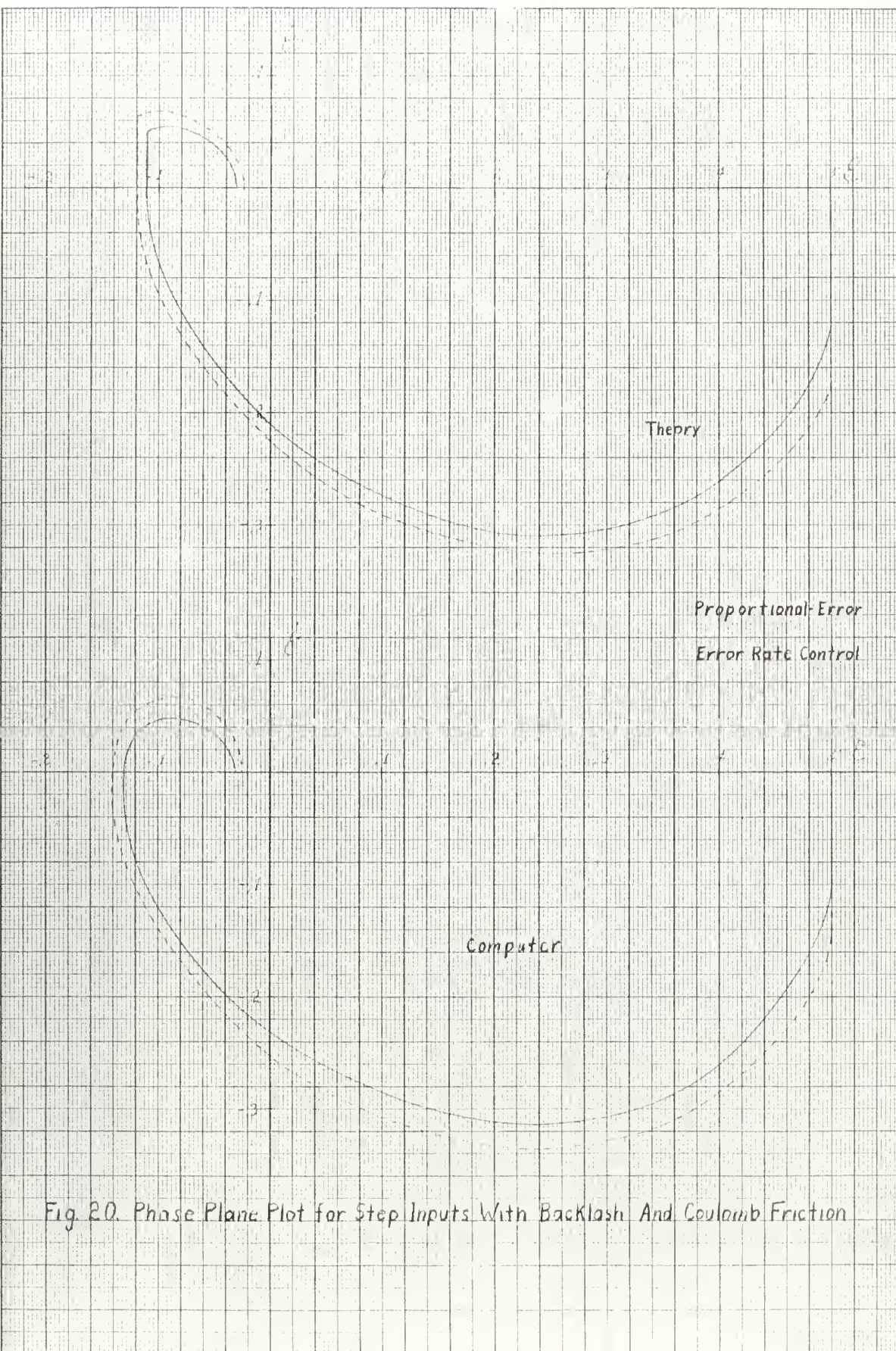


Fig. 20. Phase Plane Plot for Step Inputs With Backlash And Coulomb Friction

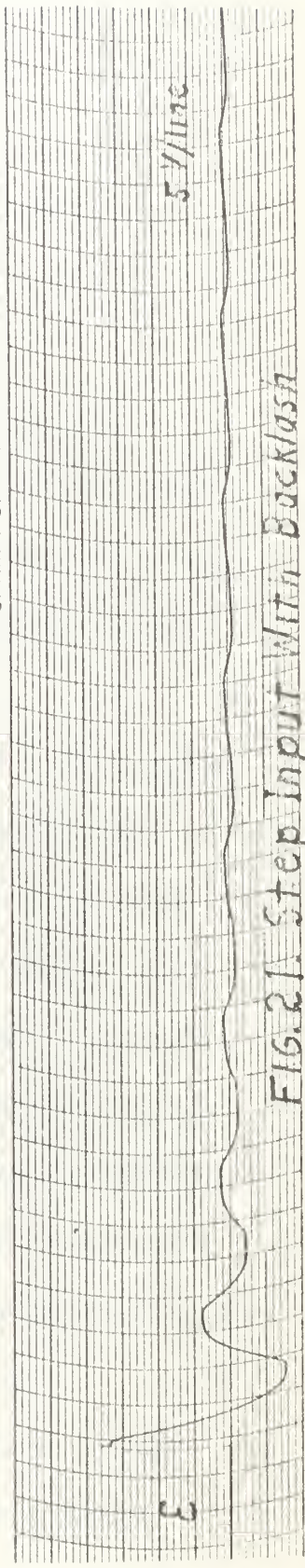
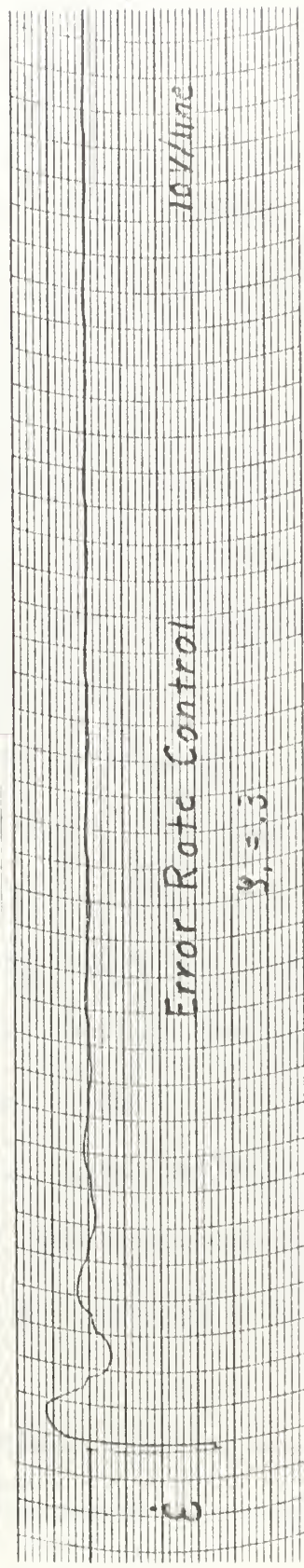
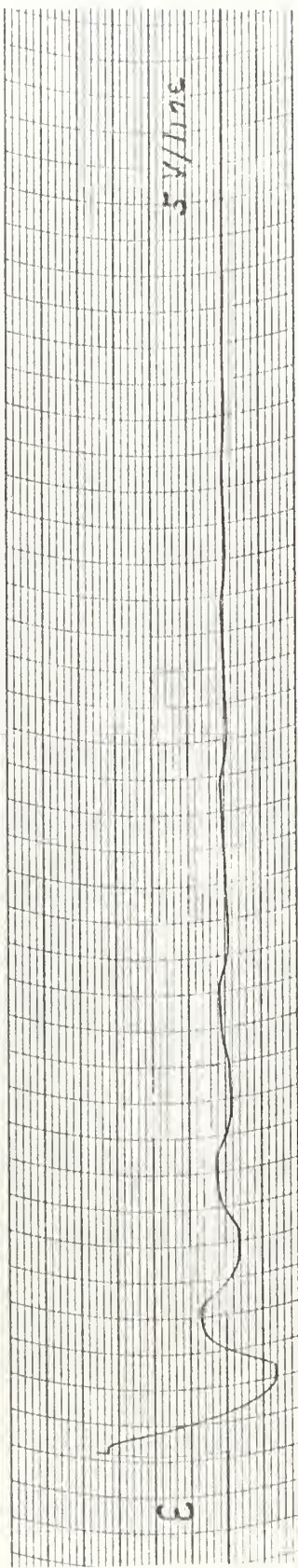
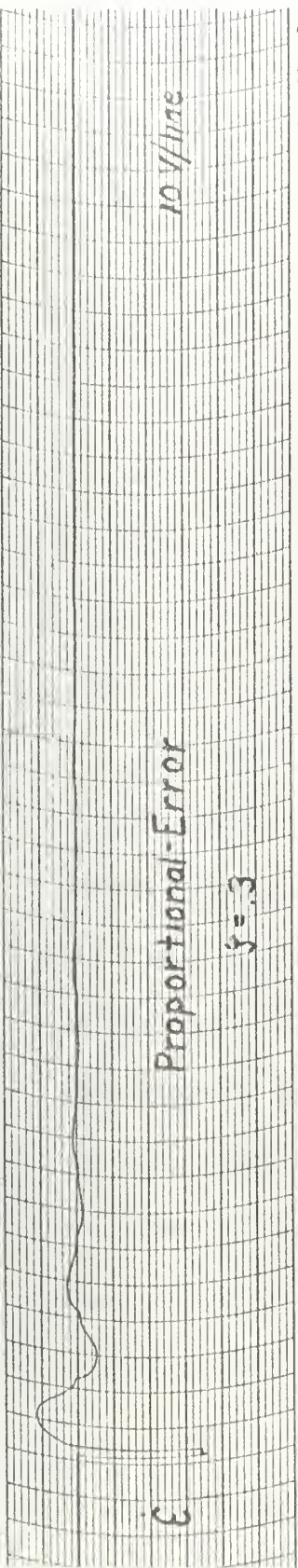


FIG. 21. Step Input With Backlash

is slightly greater than the critical value of .29. It is to be noted that it is possible to have the same instability in an actual system since any differentiation network will tend to amplify any erratic or sudden movements. Fig. 22 is the trace for an ERC system with the same parameters but with $\zeta_i = .5$. The limit cycle was eliminated by the increase in damping.

Fig. 23 is a transient response for the case with coulomb friction reacting to a small step input and illustrates the point that an ERC system will break free of coulomb friction for a step input smaller than C/K_1 while this same step input into a proportional-error system produces no results other than a static error equal to the step input.

The analog computer solutions for the ramp inputs did not have quite the accuracy of the step inputs due to the fact that it was necessary to insert a larger resistance in series with the differentiator than was used with the step inputs. This was necessary partly due to the smaller input voltage that was used to obtain sufficient problem time before the integration amplifier for the ramp input became saturated. This added resistance plus the other inherent time constants of the circuit produced considerable rounding off of many areas that should have been squared off on the Brush Recorder tapes. However, the results are definitely good enough to illustrate the points desired.

The transient response for the case in which only coulomb friction is present is shown on Fig. 24. This illustrates the point that the ERC system does not need as large an error before motion is initiated as does

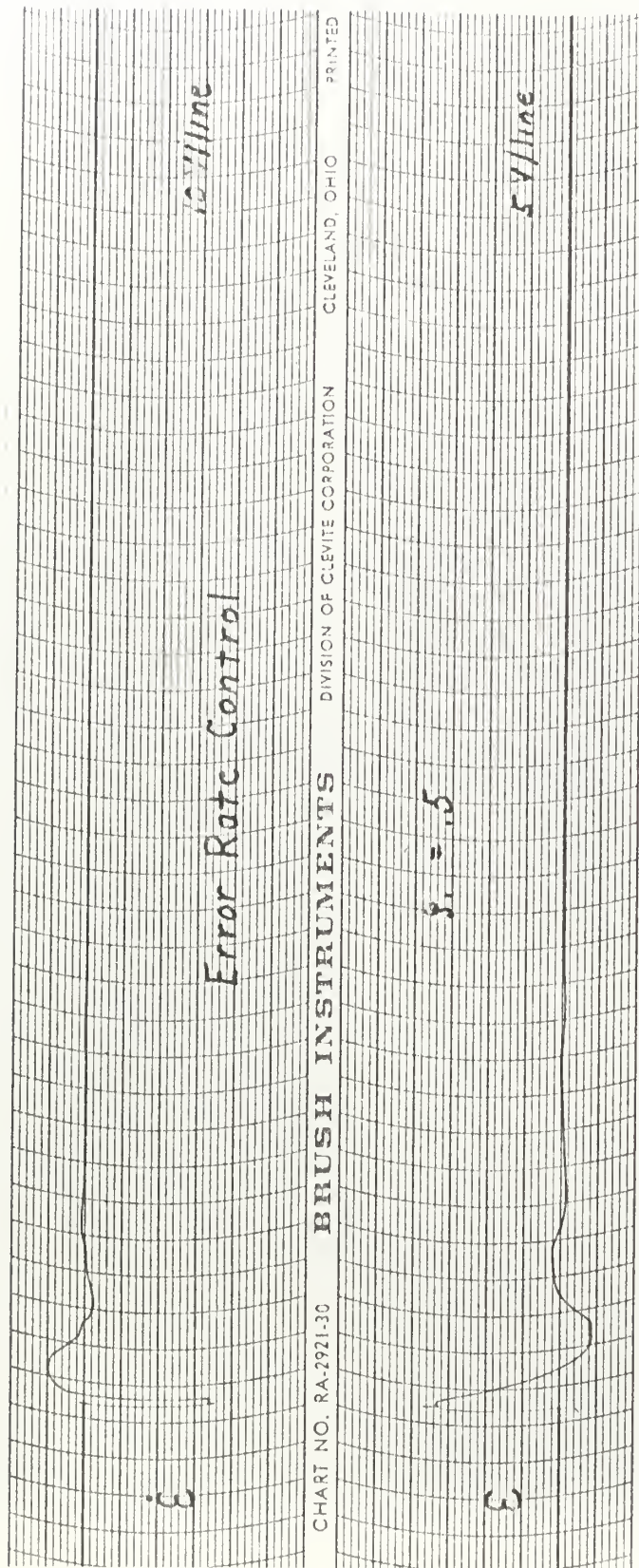


Fig. 22. Step Input With Backlash

Proportional-Error

$\xi = .3$

5 V/line

CHART NO. RA-2921-3

2 V/line

Error Rate Control

$\xi_1 = .3$

5 V/line

CHART NO. RA-2921-30 BRUSH INSTRUMENTS

Fig. 23 Small Step Input With Coulomb Friction

2 V/line

Proportional-Error

$\xi = .3$

.5 V/line

\dot{e}

CHART NO. RA-2921-30 BRUSH INSTRUMENTS

CHART NO. RA-2921-30

1 V/line

e

Error Rate Control

$\xi_1 = .3$

.5 V/line

\dot{e}

CHART NO. RA-2921-30

CHART NO. RA-2921-30

CHART NO. RA-2921-30

CHART NO. RA-2921-30

CHART NO. RA-2921-30

1 V/line

e

Fig.24. Ramp Input With Coulomb Friction

the proportional error, i.e. $(C - K_2 \theta_1)/K_1$ versus C/K_1 . The steady state error was also reduced since the value of f was reduced while keeping the damping factor constant by increasing K_2 .

When backlash is present without coulomb friction, the ERC system has its output move sooner since the motor speeds up faster due to the additional torque obtained from the $K_2 \theta_1$ term. This is illustrated in Fig. 25.

When backlash is added to the system in addition to coulomb friction, both systems add an equal increment of error before they commence output movement, but the ERC system requires less time and error to commence output movement since less error was needed to overcome the coulomb friction. The transient response illustrating this is shown in Fig. 26 and the phase plane plot in Fig. 27.

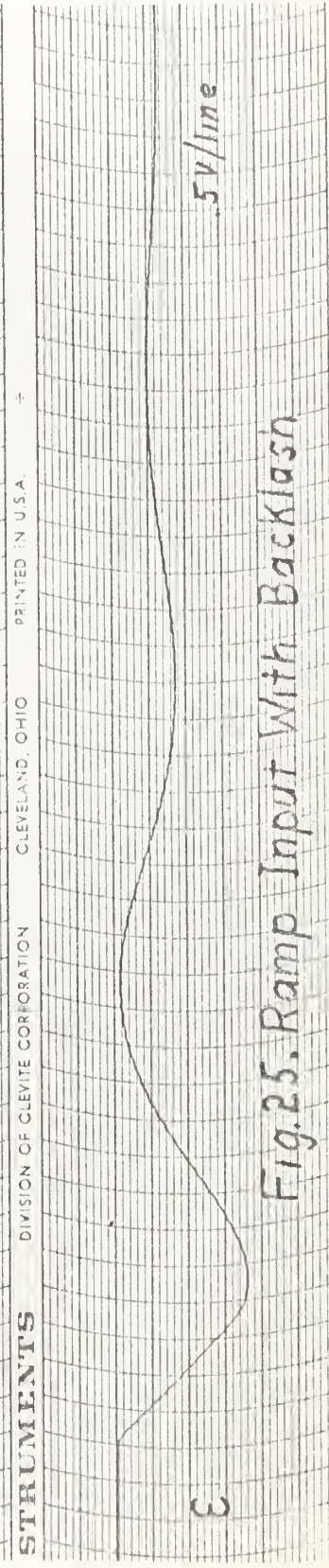
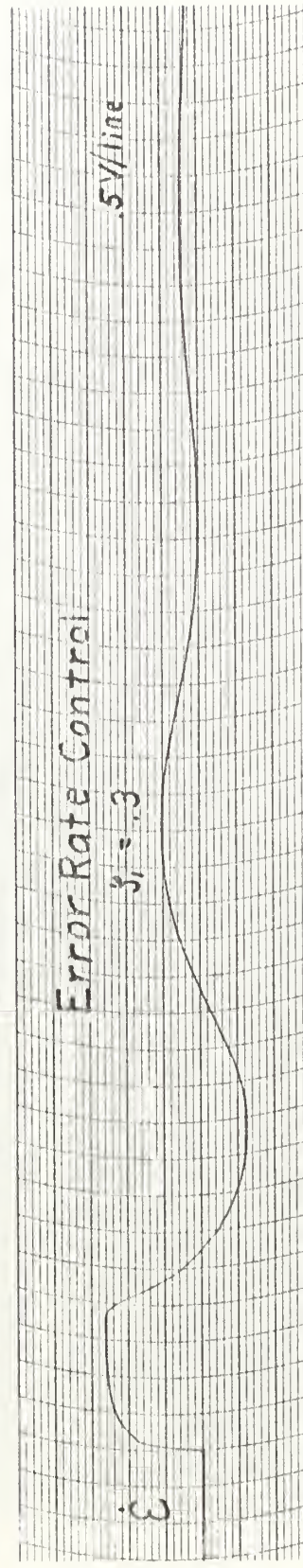
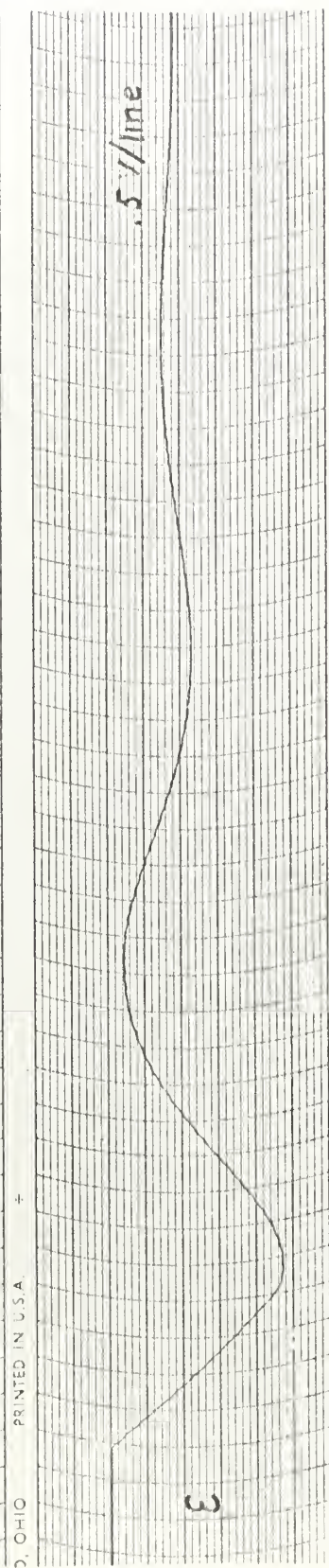
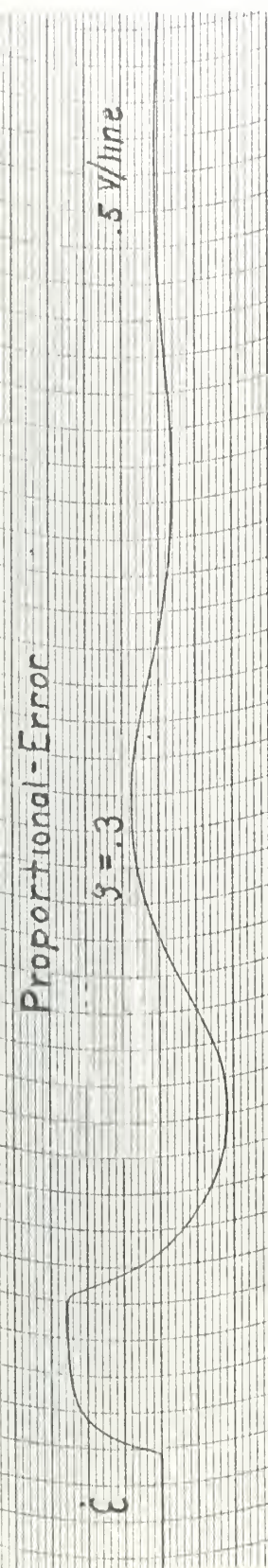


Fig.25. Ramp Input With Backlash

Proportional-Error

$$g_1 = .3$$

.5V/line

CHART NO. RA-2921-30 BRUSH INSTRUMENTS

1V/line

Error Rate Control

$$g_1 = .3$$

.5V/line

CHART NO. RA-2921-30 BRUSH INSTRUMENTS DIVISION OF CLEVELAND CORPORATION

1V/line

Fig. 26. Ramp Input With Backlash And Coulomb Friction

0.5 \dot{E}

0

0.5

1.0

1.5

E

Theory

Computer

a) Proportional Error

0.5 \dot{E}

0

0.5

1.0

1.5

E

Computer

Theory

b) Error Rate Control

Fig. 2.7. Phase Plane Plots for Ramp Inputs With Backlash and Coulomb Friction

IV. Conclusions

The use of error rate control improved on almost all the shortcomings of the proportional-error servomechanism. The basic improvements were:

1. Increased damping without an increase in the viscous friction, or conversely, the same damping with a decrease in viscous damping.
2. An increase in system speed due to the impulse of torque resulting from step inputs.
3. The ability to increase the speed of response without increasing the damping ratio by the use of gain controls alone.
4. The ability of the system to break free of coulomb friction for any size step input.
5. The decrease in steady state error for step input with coulomb friction by use of gain control.
6. Faster system response for ramp inputs due to the constant torque available.
7. A decrease in the initial error for a ramp input with coulomb friction.
8. A decrease in the steady state error for ramp inputs with coulomb friction due to gain control and possibility of decreased viscous friction.

The only drawback to the use of error rate control as was observed from the use of the Analog Computer was the increased instability of the system due to the nature of any differentiating device. This drawback can be minimized by using a slightly higher damping ratio which should

still provide most of the improvements of the ERC system with at least equivalent performance to that of the proportional-error servomechanism.

BIBLIOGRAPHY

1. G. J. Thaler and R. G. Brown, Servomechanism Analysis, McGraw-Hill Book Company, Inc., 1953.
2. J. G. Truxal, Automatic Feedback Control System Synthesis, McGraw-Hill Book Company, Inc., 1955.
3. H. Lauer, R. Lesnick and L. E. Matson, Servomechanism Fundamentals, McGraw-Hill Book Company, Inc., 1947.
4. C. A. A. Wass, Introduction to Electronic Analogue Computers, McGraw-Hill Book Company, Inc., 1956.
5. R. C. H. Wheeler, Basic Theory of the Electronic Analog Computer, Donner Scientific Company, 1955.
6. Hui S. Song, Simulation Techniques For Basic Nonlinearities in Servomechanisms, U. S. Naval Postgraduate School, 1960.

APPENDIX I

Scaling for the Analog Computer:

$$\begin{array}{ll} \text{Let} & \alpha_e \bar{E} = e \\ & \alpha_\theta \bar{\theta} = \theta \\ & \alpha_\tau \bar{\tau} = \tau \end{array} \qquad \begin{array}{ll} & \alpha_i \bar{i} = i \\ & \alpha_u \bar{u} = u \\ & \alpha_t \bar{t} = t \end{array}$$

and

$$\begin{array}{ll} \alpha_e = .006 & \alpha_i = .0001 \\ \alpha_\theta = .0007 & \alpha_u = .001 \\ \alpha_\tau = 1 & \alpha_t = 1 \end{array}$$

Amplifier # 1:

$$E = \theta_i - \theta$$

$$\begin{aligned} \bar{E} &= \bar{\theta}_i - \bar{\theta} \\ \bar{E} &= \frac{\alpha_\theta}{\alpha_e} \bar{\theta}_i - \frac{\alpha_\theta}{\alpha_e} \bar{\theta} \\ \frac{\alpha_\theta}{\alpha_e} &= \frac{a_1 R_{f1}}{R_1} = \frac{1 \cdot R_{f1}}{R_1} \end{aligned}$$

Amplifier # 2:

$$\begin{aligned} \tau_d &= K_1 E + K_2 \dot{E} \\ \tau_d \bar{\tau} &= \alpha_\tau \bar{\tau} \left(\frac{\alpha_e}{\alpha_\tau} K_1 \bar{E} + \frac{\alpha_e}{\alpha_\tau} K_2 \dot{\bar{E}} \right) \\ \frac{\alpha_e}{\alpha_\tau} K_1 &= \frac{a_5 K_{\tau 1}}{R_3} \\ \frac{\alpha_e}{\alpha_\tau} K_2 &= \frac{a_4 K_{\tau 2}}{R_4} \end{aligned}$$

Amplifier # 3:

$$\begin{aligned} \alpha_E \bar{E} &= \alpha_C \alpha_T \bar{E} \\ \bar{E} &= \alpha_T \frac{\alpha_C}{\alpha_E} \bar{E} \\ \alpha_T \frac{\alpha_C}{\alpha_E} &= \alpha_5 K_{T2} C_{M1} \end{aligned}$$

Amplifier # 4:

$$a_6 \frac{K_{T4}}{K_1} = 1 \quad (\text{sign changer})$$

Amplifier # 5:

$$\begin{aligned} \gamma_C &= \alpha_T \bar{E}_C = 1, \bar{E}_C \\ \frac{a_9 R_{T6}}{R_3} &= \text{very large number.} \\ \frac{a_{11} \frac{K_{T6} (1 + 11)}{R_{T6} + 11k}}{\bar{A}_3} &= \text{very small number.} \end{aligned}$$

Amplifier # 6:

$$\begin{aligned} \theta_M &= \frac{\gamma_d - \gamma_c}{s(f + js)} \\ \dot{\theta}_M &= s \theta_M = \frac{\gamma_d - \gamma_c}{f + js} \\ \bar{\theta}_M &= \frac{\alpha_T}{\alpha_{wf}} \frac{\bar{\gamma}_d - \bar{\gamma}_c}{1 + \alpha_c js/f} \\ \frac{\alpha_T}{\alpha_{wf}} &= \frac{a_7 R_{T5}}{21 R_6} \\ \alpha_c \frac{j}{f} &= \frac{R_{T5} C_{F1}}{L_1} \end{aligned}$$

Amplifier # 7:

$$a_{11} \frac{R_{T7}}{K_7} = 1 \quad (\text{sign changer})$$

Amplifier # 8:

$$\begin{aligned} \dot{\theta}_n &= \dot{\theta}_n \\ \dot{\theta}_n &= \frac{\dot{\theta}_n}{\alpha_\theta \alpha_t} \dot{\theta}_n \\ \frac{\dot{\theta}_n}{\alpha_\theta \alpha_t} &= \frac{\dot{\theta}_n}{R_1 C_1} \end{aligned}$$

Backlash Simulation:

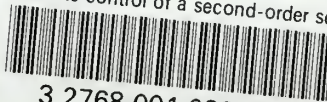
$$\Delta = \alpha_\theta \bar{E}_a = \alpha_\theta \bar{E}_t$$

Note:

Amplifier numbers refer to the numbers on the Analog
Computer circuit diagram, Fig. 17.

thesK39

Error rate control of a second-order ser



3 2768 001 03218 8

DUDLEY KNOX LIBRARY